Journal of Chemical&Engineering Data

pubs.acs.org/jced

Article

Interactions between Ethyl Lactate and Substituted Ethanols or Ethyl Acetate: Thermodynamic, FT-IR Spectroscopic, DFT Method, and PC-SAFT EoS Studies

Tammisetty Ankaiah, Sreenivasulu Karlapudi, Shaik Nagulshareef, Sridhar Battuluri, Doupati Bala Karuna Kumar, Kasibhatta Siva Kumar, Indra Bahadur,* Ariel Hernández, Faruq Mohammad, Ahmed Abdullah Soleiman, and Neelam Yugandhar Sreedhar*

Cite This: *J. Chem. Eng. Data* 2024, 69, 1423−1447

Read Online

ACCESS | Metrics & More | Article Recommendations | Supporting Information

ABSTRACT: In the present study, measurements of the experimental density (ρ), speed of sound (c), and refractive index (n_D) of binary liquid mixtures of ethyl lactate (EL) with 2-aminoethanol (2-AE), 2-chloroethanol (2-CE), and ethyl acetate (EA) have been carried out within the temperature range from 298.15 to 323.15 K with an interval of 5 K and at 0.1 MPa. Excess volume (V^E), isentropic compressibility (k_s), excess isentropic compressibility (k_s^E), and excess refractive index (n_D^E) for the above liquid mixtures were calculated from the experimental measurements and they were correlated with the Redlich−Kister equation. Also, we obtained good fitting results in the computation of the density with perturbed chain statistical associating fluid theory equation of state and predictive results in the computation of the refractive index and speed of sound with several mixing rules and Nomoto's relation, respectively. Further, we measured the Fourier-transform infrared (FT-IR) spectral data of pure liquids and their mixtures at different concentrations and simulated the molecular interactions using density functional theory (DFT) calculations for the 3 sets of binary systems with the ADF 2020.102 package at the GGA BP86-D3 level of theory with TZP. Apart from these, the type and nature of molecular interactions and structural effects were studied between the component molecules with the aid of excess thermodynamic properties, FT-IR measurements, and DFT calculations.

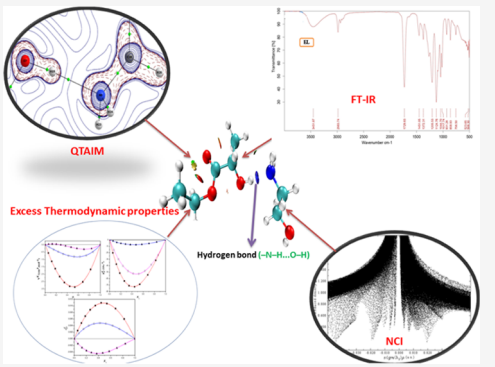

1. INTRODUCTION

In recent years, researchers are interested to study the thermodynamic and physicochemical properties of binary liquid mixtures because of their enhanced chemical separations, fluid flow, and mass transfer applications.[1−5] Based on the theoretical opinion, the study of excess thermodynamic properties of binary liquid mixtures has great significance in the investigation of the polarity, shape, and size of the component molecules and the strength of interactions prevailing between mixture components during mixing.[6−8] The liquids that were chosen in the present investigation are having many industrial applications. Ethyl lactate is a colorless liquid mainly used in the pharmaceutical industry and as a graffiti ink remover and plasticizer in polymer processing industries.[9−12] The important applications of 2-chloroethanol are manufacturing of drugs, pesticides, plasticizers, and dyes and in synthetic reactions.[13−15] 2-Aminoethanol is a colorless viscous liquid widely used in the pharmaceutical industries, for carbon dioxide absorption, and for controlling the pH in the reaction medium.[15]

An extensive survey of the literature showed that a few studies have been carried out on measurements of thermophysical and thermodynamic properties of binary mixtures containing EL with different liquids, namely, alcohols,[9] 2-alkoxyethanols,[16] C_3-alkanols,[17] aromatic/alkyl amines,[18,19] and nitrile compounds.[20,21] On the other hand, Resa et al.[22] have measured the densities, speed of sound, and refractive index for ethyl lactate with ethyl acetate at 298.15 K. As far as we know, thermophysical and excess thermodynamic properties of binary liquid mixtures of ethyl lactate with substituted ethanols and ethyl acetate at a temperature range of 298.15−323.15 K and at a pressure of 0.1 MPa with Fourier-transform infrared (FT-IR) spectroscopic and computational studies were not reported in the literature. Thus, the present study mainly focused on thermophysical properties (density, speed of sound, and refractive index) and excess thermodynamic parameters (V^E, k_s^E, and n_D^E) of EL with 2-CE, 2-AE, and

Received: June 6, 2023
Revised: January 10, 2024
Accepted: February 27, 2024
Published: March 15, 2024

https://doi.org/10.1021/acs.jced.3c00344
J. Chem. Eng. Data 2024, 69, 1423−1447

Table 1. Description of Pure Liquids

chemical name	provenance	CAS number	mass fraction purity	purification method	water content (mass fraction)
ethyl lactate	Sigma-Aldrich	97-64-3	0.997	distillation	0.0002
2-aminoethanol	SD fine chemicals	141-43-5	0.995	distillation	0.0004
2-chloroethanol	SD fine chemicals	107-07-3	0.995	distillation	0.0004
ethyl acetate	Sigma-Aldrich	141-78-6	0.999	distillation	0.0003

EA at T = 298.15−323.15 K and at 0.1 MPa together with experimental FT-IR analysis and density functional theory (DFT) calculations. Furthermore, we have used perturbed chain statistical associating fluid theory equation of state (PC-SAFT EoS) for modeling the density of the binary mixtures. Nomoto's relation (NR) coupled to PC-SAFT EoS was used for modeling the speed of sound of mixtures using a predictive approach, and PC-SAFT EoS + four different mixing rules were used for modeling the refractive index of mixtures.

2. EXPERIMENTAL AND/OR COMPUTATIONAL METHODS

2.1. Materials. The liquids utilized in the present study, i.e., ethyl lactate and ethyl acetate, were purchased from Sigma-Aldrich, India and the remaining two liquids, i.e., 2-aminoethanol and 2-chloroethanol, were purchased from SD Fine Chemicals, India. The mass fraction purities of all of the above chemicals were obtained from the suppliers, and the water content was determined by using the Analab (Micro Aqua Cal 100) Karl Fischer Titrator together with Karl Fisher reagent from Merck. This data is given in Table 1.

2.2. Apparatus and Procedure. The binary mixtures of EL with substituted ethanols or ethyl acetate were prepared by using an Afcoset weighing balance (ER-120A, India) with a precision of 0.1 mg. The uncertainty of the mole fraction was 0.0005. The densities and speed of sound were measured with Anton Paar, DSA 5000 M, Austria, and the refractive index was determined using an automated refractometer (Anton Paar, Abbemat 3200, Austria). The details of measurements and the calibration of the instruments were described earlier.[23] The uncertainties were estimated for density, speed of sound, and refractive index measurements within 0.0009 g cm^{-3}, 2.91 m s^{-2}, and 0.0006, respectively. Figure S1 illustrates the comparison of the experimental density, speed of sound, and refractive index of pure liquids together with the available literature data[1,9,13,15−17,19−22,24−37] at all of the studied temperatures (Table 2). The range of deviations from the literature of pure liquids is within the reported uncertainties of these properties except a few (2-chloroethanol,[31] 2-aminoethanol,[15] ethyl acetate),[27,35,36] which show high deviation for only speed of sound. This might be due to the different instruments used with low accuracy as compared to the instrument used in this study as well as the purity of pure liquids. The maximum deviation in measured properties such as density, speed of sound, and refractive index was 0.3, 0.8, and 0.2%, respectively. The uncertainty in excess molar volume, excess isentropic compressibility, and excess refractive index was 0.005 cm^3 mol^{-1}, 0.2 T Pa^{-1}, and 0.0009, respectively.

2.3. PC-SAFT EoS Model. PC-SAFT EoS has been widely used in literature in order to model the physical properties of mixtures. In the Gross and Sadowski articles[38,39] can be reviewing the equations related to PC-SAFT EoS. The advantage of using a molecular equation of state like PC-SAFT is that the association part can be considered between molecules of the same type and of different types. The association schemes for each pure fluid are (x)ps − (y)ns, where ps is the positive site and ns is the negative site, i.e., the proton donor is the positive site and the proton acceptor is the negative site. Ethyl lactate will be modeled as (1)ps − (3)ns because it has three oxygen atoms and one hydrogen atom. 2-Aminoethanol, possessing the OH group and the NH_2 group, will be modeled using a 4C scheme or (2)ps − (2)ns, i.e., one negative site on the oxygen atom and another on the nitrogen atom, while a positive site was placed on the hydrogen atom bonded to the OH group and the other positive site will be placed in hydrogen atoms bonded to nitrogen. For the 2-chloroethanol fluid, a 2B or (1)ps − (1)ns scheme was considered, i.e., one positive site in the hydrogen atom and one negative site in the oxygen atom. Finally, ethyl acetate having two oxygen atoms was modeled as (0)ps − (2)ns. Therefore, in the case of the ethyl lactate + 2-aminoethanol and ethyl lactate + 2-chloroethanol mixtures, we have considered a cross-association between positive and negative sites, while to consider the cross-association between ethyl lactate and ethyl acetate, the Kleiner and Sadowski approach was used.[40]

The speed of sound was modeled using Nomoto's relation[41] and the refractive index was modeled using the Lorentz−Lorenz (LL), Gladstone−Dale (GD), Laplace (LP), and Eykman (EK) mixing rules. The advantage of using these models is that both the speed of sound and the refractive index are predicted properties using these models combined with PC-SAFT EoS. The details of the equations to obtain the speed of sound and the refractive index were mentioned earlier.[41,42]

2.4. Computational Details. In the current work, we have simulated the theoretical intermolecular bonding interactions using DFT calculations for the 3 sets of binary solutions. We have started with geometry optimizations followed by studying the interactions between EL and 2-aminoethanol, followed by the interactions between ethyl lactate and 2-chloroethanol and EL and ethyl acetate using the ADF 2020.102 package.[43] The geometry of the binary systems was optimized at the GGA BP86-D3 (BJ) level of theory with TZP with the following conditions applied: a Becke[44,45] numerical of a good quality integration grid, a 1 × 10^{-6} hartree gradient convergence for the optimization of geometry, and a SCF convergence of 1 × 10^{-6} hartree for each of the three relevant interacting molecular pairs in order to accurately describe the bonding interactions and their corresponding energies.

3. RESULTS AND DISCUSSION

3.1. Volumetric Properties. Excess volume data of three binary mixtures, V^E, were calculated by using the experimental densities based on eq 1 and the values are given in Table 3.

$$V^E = \frac{\sum_{i=1}^{n} x_i M_i}{\rho_m} - \sum_{i=1}^{n} \frac{x_i M_i}{\rho_i} \quad (1)$$

https://doi.org/10.1021/acs.jced.3c00344
J. Chem. Eng. Data 2024, 69, 1423−1447

Table 2. Experimental and Literature Densities (ρ), Speed of Sound (c), and Refractive Index (n_D) of Pure Solvents at T = 298.15−323.15 K and at Pressure p = 0.1 MPa[a]

		ρ/(g cm^{-3})		c/(m s^{-1})		n_D	
chemical name	temperature (K)	exp.	lit.	exp.	lit.	exp.	lit.
ethyl lactate	298.15	1.0284	1.028392[24]	1279.86	1279.34[9]	1.4104	1.41076[24]
			1.02845[9]		1277[22]		1.41050[22]
			1.02802[22]		1277[26]		1.41057[26]
			1.0286[26]				
	303.15	1.0229	1.02288[16]	1261.20	1261.2[17]	1.4082	1.40843[24]
			1.02358[17]		1261.1[16]		1.40820[20]
			1.022918[24]		1261.1[19]		1.40820[21]
			1.0236[19]		1260.35[20]		
			1.02281[20]		1260.39[21]		
			1.02293[21]				
	308.15	1.0174	1.01739[16]	1242.06	1243.8[17]	1.4059	1.40610[24]
			1.01656[17]		1243.8[16]		
			1.017420[24]		1243.8[19]		
			1.0166[19]				
	313.15	1.0119	1.01183[16]	1224.00	1224.8[17]	1.4036	1.40374[24]
			1.01183[17]		1224.8[16]		1.40361[20]
			1.011902[24]		1224.8[19]		1.40367[21]
			1.0118[19]		1222.62[20]		
			1.01191[20]		1222.60[21]		
			1.01191[21]				
	318.15	1.0064	1.00631[16]	1205.38	1206.9[17]	1.4014	1.40136[24]
			1.00631[17]		1206.9[16]		
			1.006358[24]				
	323.15	1.0008	1.000789[24]	1186.90	1185.61[21]	1.3991	1.39898[24]
			1.00078[21]		1185.58[20]		1.39899[20]
			1.00073[20]				1.39895[21]
2-chloroethanol	298.15	1.1976	1.1976[27]	1360.2	1359[28]	1.4393	1.4402[27]
			1.19709[13]		1358[29]		1.4416[28]
			1.1980[28]		1363[27]		1.4411[29]
			1.2009[29]		1357.6[30]		
			1.1963[30]				
			1.19623[1]				
	303.15	1.1925	1.19025[13]	1340.30	1342.8[15]	1.4372	1.4373[27]
			1.1921[27]		1343.6[31]		1.4385[28]
			1.1924[28]				1.4380[29]
			1.1925[29]				
			1.19212[15]				
			1.19054[1]				
			1.1905[31]				
	308.15	1.1867	1.1866[27]	1330.49	1328.9[15]	1.4350	1.4342[27]
			1.1854[28]		1329.9[30]		1.4326[28]
			1.1871[29]				1.4326[29]
			1.18526[15]				
			1.1849[30]				
			1.18487[1]				
	313.15	1.1784	1.17679[13]	1316.07	1315.5[15]	1.4329	
			1.17837[15]		1315.0[31]		
			1.1792[31]				
	318.15	1.1737	1.1738[30]	1302.00	1301.2[15]	1.4307	
			1.17087[15]		1300.2[30]		
	323.15	1.1703	1.16801[1]	1288.10		1.4286	
2-aminoethanol	298.15	1.0121	1.012020[32]	1718.68	1719.23[32]	1.4525	1.452[25]
			1.01253[33]		1719.2[34]		
			1.01198[34]		1717.2[25]		
			1.0133[25]				
	303.15	1.0081	1.008002[32]	1702.78	1703.09[32]	1.4506	
			1.00847[33]		1702.1[34]		
			1.00802[34]		1704.9[15]		

https://doi.org/10.1021/acs.jced.3c00344
J. Chem. Eng. Data 2024, 69, 1423−1447

Table 2. continued

chemical name	temperature (K)	ρ/(g cm^{-3}) exp.	ρ/(g cm^{-3}) lit.	c/(m s^{-1}) exp.	c/(m s^{-1}) lit.	n_D exp.	n_D lit.
			1.00872[15]				
	308.15	1.0041	1.004024[32]	1686.05	1686.79[32]	1.4487	
			1.00449[33]		1690.1[15]		
			1.00477[15]				
	313.15	1.0007	1.000037[32]	1670	1670.54[32]	1.4468	
			1.00050[33]		1670.1[34]		
			1.00006[34]		1675.2[15]		
			1.00057[15]				
	318.15	0.9960	0.996029[32]	1654.01	1654.19[32]	1.4449	
			0.99639[33]		1659.4[15]		
			0.99604[15]				
	323.15	0.9922	0.992014[32]	1637.58	1637.86[32]	1.4429	
			0.99241[33]		1637.2[34]		
			0.99205[34]				
ethyl acetate	298.15	0.8944	0.89429[22]	1138.78	1138[22]	1.3700	1.36978[22]
			0.89456[35]		1145[35]		1.3710[27]
			0.8948[27]		1148[27]		1.371[36]
			0.8928[36]		1142[36]		1.37014[37]
			0.89448[37]		1139.68[37]		
	303.15	0.8883	0.88890[35]	1116.62	1119[35]	1.3675	1.3681[27]
			0.8887[27]		1117.14[37]		1.36752[37]
			0.88834[37]				
	308.15	0.8821	0.8826[35]	1094.44	1098[35]	1.3649	1.3654[27]
			0.8827[27]		1094.68[37]		1.36481[37]
			0.88215[37]				
	313.15	0.8759	0.8759[35]	1072.35	1081[35]	1.3625	1.36209[37]
			0.87592[37]		1072.33[37]		
	318.15	0.8697	0.8696[35]	1050.4	1058[35]	1.3592	1.35938[37]
			0.86963[37]		1050.13[37]		
	323.15	0.8633	0.86329[37]	1028.61	1027.99[37]	1.3567	1.35664[37]

[a]Standard uncertainties u are $u(T) = 0.02$ K and $u(p) = 0.04$ MPa, and the combined expanded uncertainties Uc in mole fraction, density, speed of sound, refractive index, excess molar volume, excess isentropic compressibility, and excess refractive index are Uc(x) = 0.0005, Uc(ρ) = 0.0009 g cm^{-3}, Uc(c) = 2.91 m s^{-1}, Uc(n_D) = 0.0006, Uc(V^E) = 0.005 cm^3·mol^{-1}, Uc(k_s^E) = 0.2 T Pa^{-1}, and Uc(n_D^E) = 0.0009, respectively (0.95 level of confidence).

Here, ρ_m refers to the density of the mixture. M_i, ρ_i, and x_i are the molar mass, density, and mole fraction of component i, respectively. The calculated V^E values plotted against the mole fraction of ethyl lactate at 298.15 K for three binary systems are shown in Figure 1.

The V^E values are negative for binary mixtures of EL + 2-aminoethanol or ethyl acetate and the inversion sign was observed for EL + 2-chloroethanol at 298.15 K. It is well known that substituted ethanol (2-AE and 2-CE) molecules are associated through intramolecular hydrogen bonding interactions in the pure state. Mixing of these liquids with ethyl lactate would induce the mutual disruption of intramolecular hydrogen-bonded interactions in pure-component molecules and as a result, new intermolecular hydrogen bonds were formed between the hydrogen atom of the $-NH_2$ group of 2-AE and the carbonyl group of EL (−C═O···−H−N−) and hydrogen atom of the −OH group in the 2-CE molecule and the carbonyl group of EL (−C═O···−H−O−). Moreover, the negative V^E data of the EL + EA binary system suggested a better compaction between ethyl lactate and ethyl acetate through the molecular interactions in liquid mixtures than that of pure liquids. Hence, the algebraic V^E data follow the order: EL > 2-AE > EA > 2-CE. As the temperature increases, the absolute V^E values increase in the three binary liquid mixtures due to the enhancement of the number of free dipoles, thereby increasing intermolecular interactions between component molecules.[24,46]

Furthermore, the experimental density, speed of sound, and refractive index data for the ethyl lactate + ethyl acetate binary system were compared with the literature data[22] at 298.15 K and is given in Figure 2. A similar trend with noticeable deviation was observed for all measured properties. The maximum deviation between the experimental and literature values for density, speed of sound, and refractive index is 8.9, 6.9, and 1.9%, respectively. This may be due to the human error in the preparation of the sample and the high accuracy of the instrument used in this work compared to the literature.[22]

The excess isentropic compressibility (k_s^E) with respect to ideality was calculated through the following equation

$$k_s^E = k_s - k_s^{id} \tag{2}$$

The isentropic compressibilities (k_s) were calculated from the Newton−Laplace equation as follows

$$k_s = \frac{1}{c^2\rho} \tag{3}$$

where ρ and c represent the density and speed of sound of the binary mixtures, respectively. The ideal isentropic compresibi-

https://doi.org/10.1021/acs.jced.3c00344
J. Chem. Eng. Data 2024, 69, 1423−1447

Table 3. Experimental Results of the Density (ρ), Speed of Sound (c), and Refractive Index (n_D) of the Binary Mixtures Along with Calculated Excess Properties (V^E, k_s^E, and n_D^E) at All of the Investigated Temperatures (298.15−323.15 K) and at Pressure p = 0.1 MPa[a]

x_1	ρ (g cm^{-3})	V^E (cm^3 mol^{-1})	c (m s^{-1})	κ_s (T Pa^{-1})	k_s^E(T Pa^{-1})	n_D	n_D^E
			Ethyl Lactate + 2-Aminoethanol				
T = 298.15 K							
0.0000	1.0121	0.000	1718.68	334.48	0.0	1.4525	0.0000
0.0570	1.0229	−0.563	1689.00	342.69	−20.1	1.4526	0.0044
0.1190	1.0329	−1.129	1656.78	352.69	−37.7	1.4523	0.0084
0.1821	1.0411	−1.629	1624.83	363.81	−51.6	1.4517	0.0117
0.2640	1.0491	−2.162	1583.28	380.24	−63.8	1.4502	0.0148
0.3470	1.0544	−2.558	1542.80	398.46	−71.0	1.4480	0.0167
0.4446	1.0573	−2.826	1495.70	422.77	−72.7	1.4447	0.0176
0.5380	1.0572	−2.870	1452.50	448.34	−68.8	1.4406	0.0171
0.6818	1.0524	−2.521	1390.45	491.47	−54.2	1.4330	0.0143
0.8238	1.0434	−1.679	1335.30	537.51	−31.8	1.4238	0.0091
1.0000	1.0284	0.000	1279.86	593.63	0.0	1.4104	0.0000
T = 303.15 K							
0.0000	1.0081	0.000	1702.78	342.11	0.0	1.4506	0.0000
0.0570	1.0190	−0.586	1676.23	349.25	−22.8	1.4507	0.0045
0.1190	1.0290	−1.164	1646.80	358.33	−42.8	1.4505	0.0086
0.1821	1.0373	−1.682	1616.02	369.15	−58.3	1.4499	0.0119
0.2640	1.0453	−2.233	1576.18	385.08	−72.6	1.4484	0.0150
0.3470	1.0505	−2.646	1535.29	403.84	−80.5	1.4463	0.0170
0.4446	1.0534	−2.928	1487.05	429.28	−82.4	1.4429	0.0179
0.5380	1.0532	−2.980	1443.80	455.48	−79.0	1.4389	0.0175
0.6818	1.0482	−2.626	1378.00	502.43	−62.0	1.4312	0.0147
0.8238	1.0387	−1.757	1320.30	552.28	−36.8	1.4219	0.0094
1.0000	1.0229	0.000	1261.20	614.58	0.0	1.4082	0.0000
T = 308.15 K							
0.0000	1.0041	0.000	1686.05	350.32	0.0	1.4487	0.0000
0.0570	1.0151	−0.605	1660.78	357.16	−24.9	1.4489	0.0046
0.1190	1.0251	−1.201	1631.08	366.66	−46.1	1.4488	0.0089
0.1821	1.0334	−1.735	1601.74	377.17	−63.4	1.4482	0.0123
0.2640	1.0414	−2.308	1561.94	393.58	−78.9	1.4468	0.0155
0.3470	1.0467	−2.738	1521.02	412.97	−87.6	1.4447	0.0176
0.4446	1.0495	−3.036	1473.33	438.94	−90.4	1.4413	0.0185
0.5380	1.0492	−3.095	1428.40	467.13	−86.2	1.4373	0.0181
0.6818	1.0439	−2.737	1362.56	516.00	−68.7	1.4294	0.0151
0.8238	1.0340	−1.838	1303.60	569.12	−41.4	1.4199	0.0097
1.0000	1.0174	0.000	1242.06	637.10	0.0	1.4059	0.0000
T = 313.15 K							
0.0000	1.0007	0.000	1670.00	358.33	0.0	1.4468	0.0000
0.0570	1.0116	−0.623	1645.21	365.20	−27.6	1.4471	0.0048
0.1190	1.0217	−1.238	1616.90	374.39	−51.6	1.4470	0.0091
0.1821	1.0300	−1.790	1584.02	386.96	−68.9	1.4465	0.0126
0.2640	1.0379	−2.384	1541.41	405.50	−84.3	1.4452	0.0160
0.3470	1.0431	−2.832	1502.25	424.79	−94.7	1.4431	0.0181
0.4446	1.0458	−3.145	1454.63	451.87	−97.8	1.4397	0.0190
0.5380	1.0454	−3.213	1409.00	481.84	−92.7	1.4356	0.0186
0.6818	1.0397	−2.851	1344.02	532.46	−74.3	1.4276	0.0155
0.8238	1.0293	−1.923	1286.90	586.62	−46.3	1.4179	0.0100
1.0000	1.0119	0.000	1224.00	659.62	0.0	1.4036	0.0000
T = 318.15 K							
0.0000	0.9960	0.000	1654.01	366.99	0.0	1.4449	0.0000
0.0570	1.0071	−0.642	1633.00	372.34	−29.1	1.4453	0.0049
0.1190	1.0173	−1.277	1606.84	380.73	−54.1	1.4452	0.0092
0.1821	1.0256	−1.847	1577.50	391.81	−73.5	1.4448	0.0129
0.2640	1.0337	−2.463	1539.98	407.91	−92.3	1.4435	0.0163
0.3470	1.0390	−2.929	1499.84	427.87	−103.4	1.4414	0.0184
0.4446	1.0417	−3.258	1450.00	456.60	−106.5	1.4380	0.0194
0.5380	1.0412	−3.335	1404.08	487.19	−102.5	1.4339	0.0190
0.6818	1.0353	−2.970	1335.11	541.90	−82.9	1.4259	0.0160

https://doi.org/10.1021/acs.jced.3c00344
J. Chem. Eng. Data 2024, 69, 1423−1447

Table 3. continued

x_1	ρ (g cm^{-3})	V^E (cm^3 mol^{-1})	c (m s^{-1})	κ_s (T Pa^{-1})	k_s^E(T Pa^{-1})	n_D	n_D^E
0.8238	1.0245	−2.011	1273.25	602.09	−51.7	1.4160	0.0102
1.0000	1.0064	0.000	1205.38	683.91	0.0	1.4014	0.0000
T = 323.15 K							
0.0000	0.9922	0.000	1637.58	375.83	0.0	1.4429	0.0000
0.0570	1.0033	−0.660	1614.00	382.60	−31.0	1.4433	0.0050
0.1190	1.0135	−1.315	1587.01	391.75	−58.2	1.4434	0.0095
0.1821	1.0219	−1.904	1558.53	402.87	−79.9	1.4430	0.0132
0.2640	1.0300	−2.543	1519.87	420.29	−99.9	1.4418	0.0168
0.3470	1.0352	−3.028	1479.00	441.61	−111.5	1.4398	0.0190
0.4446	1.0379	−3.375	1431.64	470.10	−116.4	1.4364	0.0200
0.5380	1.0372	−3.462	1385.05	502.57	−111.5	1.4323	0.0197
0.6818	1.0310	−3.095	1317.00	559.19	−90.8	1.4241	0.0164
0.8238	1.0198	−2.106	1254.11	623.46	−55.9	1.4141	0.0106
1.0000	1.0008	0.000	1186.90	709.30	0.0	1.3991	0.0000
			Ethyl Lactate + 2-Chloroethanol				
T = 298.15 K							
0.0000	1.1976	0.000	1360.20	451.30	0.0	1.4393	0.0000
0.0615	1.1798	0.041	1350.66	464.61	−1.7	1.4360	−0.0004
0.1283	1.1626	0.055	1342.48	477.26	−3.9	1.4329	−0.0006
0.2018	1.1458	0.039	1334.00	490.43	−5.4	1.4298	−0.0007
0.2826	1.1294	−0.005	1325.77	503.75	−6.6	1.4269	−0.0007
0.3702	1.1136	−0.076	1317.65	517.21	−7.3	1.4241	−0.0007
0.4701	1.0975	−0.170	1309.50	531.34	−7.5	1.4214	−0.0004
0.5757	1.0821	−0.252	1301.66	545.35	−6.9	1.4189	−0.0002
0.7035	1.0650	−0.308	1293.75	560.98	−5.6	1.4162	0.0001
0.8404	1.0478	−0.263	1286.38	576.74	−3.3	1.4135	0.0002
1.0000	1.0284	0.000	1279.86	593.63	0.0	1.4104	0.0000
T = 303.15 K							
0.0000	1.1925	0.000	1340.30	466.81	0.0	1.4372	0.0000
0.0615	1.1748	0.030	1333.07	478.99	−2.8	1.4340	−0.0003
0.1283	1.1577	0.033	1325.46	491.66	−5.0	1.4309	−0.0004
0.2018	1.1409	0.018	1318.29	504.37	−7.3	1.4279	−0.0005
0.2826	1.1245	−0.033	1310.48	517.83	−8.7	1.4250	−0.0005
0.3702	1.1086	−0.106	1302.41	531.75	−9.4	1.4223	−0.0003
0.4701	1.0924	−0.192	1294.14	546.57	−9.5	1.4195	−0.0002
0.5757	1.0769	−0.270	1286.19	561.34	−8.9	1.4171	0.0002
0.7035	1.0597	−0.321	1277.39	578.33	−7.2	1.4142	0.0003
0.8404	1.0424	−0.271	1269.16	595.55	−4.3	1.4114	0.0004
1.0000	1.0229	0.000	1261.20	614.58	0.0	1.4082	0.0000
T = 308.15 K							
0.0000	1.1867	0.000	1330.49	476.02	0.0	1.435	0.0000
0.0615	1.1693	0.019	1322.46	489.02	−3.4	1.4319	−0.0001
0.1283	1.1522	0.020	1314.18	502.53	−6.1	1.4289	−0.0002
0.2018	1.1355	−0.008	1305.74	516.52	−8.4	1.4259	−0.0003
0.2826	1.1192	−0.061	1297.14	531.04	−10.2	1.4230	−0.0002
0.3702	1.1034	−0.137	1288.55	545.85	−11.3	1.4202	−0.0002
0.4701	1.0871	−0.222	1279.58	561.81	−11.6	1.4176	0.0002
0.5757	1.0715	−0.297	1270.68	577.99	−10.9	1.4149	0.0003
0.7035	1.0542	−0.336	1261.04	596.50	−9.0	1.4121	0.0005
0.8404	1.0370	−0.281	1251.56	615.65	−5.5	1.4092	0.0004
1.0000	1.0174	0.000	1242.06	637.10	0.0	1.4059	0.0000
T = 313.15 K							
0.0000	1.1784	0.000	1316.07	489.96	0.0	1.4329	0.0000
0.0615	1.1614	0.010	1303.15	507.04	−4.0	1.4297	−0.0002
0.1283	1.1448	0.002	1291.46	523.75	−7.3	1.4268	−0.0002
0.2018	1.1284	−0.030	1281.02	540.03	−10.1	1.4239	−0.0001
0.2826	1.1124	−0.086	1271.64	555.93	−12.4	1.4209	−0.0002
0.3702	1.0968	−0.162	1262.82	571.72	−13.6	1.4183	0.0001
0.4701	1.0808	−0.244	1254.65	587.78	−14.2	1.4155	0.0003
0.5757	1.0654	−0.316	1246.89	603.71	−13.2	1.4128	0.0004
0.7035	1.0483	−0.350	1238.90	621.50	−10.8	1.4099	0.0006

https://doi.org/10.1021/acs.jced.3c00344
J. Chem. Eng. Data 2024, 69, 1423−1447

Table 3. continued

x_1	ρ (g cm^{-3})	V^E (cm^3 mol^{-1})	c (m s^{-1})	κ_s (T Pa^{-1})	k_s^E(T Pa^{-1})	n_D	n_D^E
0.8404	1.0312	−0.286	1231.38	639.54	−6.6	1.4070	0.0005
1.0000	1.0119	0.000	1224.00	659.62	0.0	1.4036	0.0000
T = 318.15 K							
0.0000	1.1737	0.000	1302.00	502.61	0.0	1.4307	0.0000
0.0615	1.1566	0.005	1293.77	516.52	−4.8	1.4279	0.0002
0.1283	1.1400	−0.008	1285.35	530.95	−8.9	1.4250	0.0002
0.2018	1.1236	−0.046	1276.32	546.33	−12.1	1.4221	0.0003
0.2826	1.1075	−0.103	1267.43	562.10	−14.7	1.4194	0.0005
0.3702	1.0918	−0.179	1257.97	578.78	−15.9	1.4166	0.0006
0.4701	1.0757	−0.261	1248.27	596.63	−16.4	1.4138	0.0008
0.5757	1.0602	−0.331	1238.44	614.99	−15.3	1.411	0.0008
0.7035	1.0429	−0.359	1227.32	636.55	−12.3	1.408	0.0008
0.8404	1.0257	−0.291	1216.56	658.73	−7.5	1.4049	0.0006
1.0000	1.0064	0.000	1205.38	683.91	0.0	1.4014	0.0000
T = 323.15 K							
0.0000	1.1703	0.000	1288.10	515.00	0.0	1.4286	0.0000
0.0615	1.1530	0.002	1277.32	531.56	−5.6	1.4258	0.0002
0.1283	1.1363	−0.018	1266.76	548.45	−10.1	1.4230	0.0004
0.2018	1.1197	−0.063	1256.96	565.26	−14.2	1.4202	0.0005
0.2826	1.1033	−0.120	1247.14	582.73	−17.0	1.4174	0.0007
0.3702	1.0875	−0.199	1237.43	600.55	−18.5	1.4147	0.0009
0.4701	1.0711	−0.280	1227.78	619.37	−19.0	1.4118	0.0010
0.5757	1.0553	−0.350	1218.00	638.72	−17.5	1.4090	0.0011
0.7035	1.0378	−0.376	1207.28	661.08	−13.8	1.4059	0.0010
0.8404	1.0204	−0.301	1197.09	683.88	−8.3	1.4027	0.0007
1.0000	1.0008	0.000	1186.90	709.30	0.0	1.3991	0.0000
			Ethyl Lactate + Ethyl Acetate				
T = 298.15 K							
0.0000	0.8944	0.000	1138.78	862.15	0.0	1.3700	0.0000
0.0750	0.9075	−0.169	1153.12	828.70	−15.5	1.3747	0.0012
0.1542	0.9209	−0.330	1169.08	794.49	−29.9	1.3792	0.0021
0.2382	0.9345	−0.474	1184.77	762.31	−40.4	1.3836	0.0028
0.3272	0.9487	−0.635	1201.00	730.78	−48.4	1.3878	0.0032
0.4218	0.9628	−0.740	1217.09	701.19	−52.4	1.3918	0.0032
0.5225	0.9768	−0.801	1233.11	673.24	−52.7	1.3957	0.0030
0.6299	0.9909	−0.809	1248.04	647.92	−48.3	1.3994	0.0025
0.7448	1.0046	−0.727	1261.10	625.93	−38.4	1.4031	0.0019
0.8678	1.0174	−0.492	1273.10	606.46	−23.7	1.4068	0.0011
1.0000	1.0284	0.000	1279.86	593.63	0.0	1.4104	0.0000
T = 303.15 K							
0.0000	0.8883	0.000	1116.62	902.9	0.0	1.3675	0.0000
0.0750	0.9017	−0.203	1130.80	867.3	−17.2	1.3725	0.0015
0.1542	0.9150	−0.352	1145.90	832.3	−31.5	1.3770	0.0024
0.2382	0.9289	−0.513	1161.75	797.7	−43.3	1.3815	0.0031
0.3272	0.9430	−0.666	1177.65	764.6	−51.2	1.3857	0.0035
0.4218	0.9572	−0.780	1194.36	732.4	−56.0	1.3897	0.0035
0.5225	0.9714	−0.853	1211.09	701.8	−56.8	1.3937	0.0034
0.6299	0.9855	−0.860	1227.09	673.9	−52.5	1.3974	0.0028
0.7448	0.9992	−0.764	1241.07	649.8	−41.9	1.4011	0.0022
0.8678	1.0121	−0.528	1253.76	628.6	−25.9	1.4046	0.0011
1.0000	1.0229	0.000	1261.20	614.58	0.0	1.4082	0.0000
T = 308.15 K							
0.0000	0.8821	0.000	1094.44	946.42	0.0	1.3649	0.0000
0.0750	0.8956	−0.200	1108.59	908.60	−17.6	1.3701	0.0017
0.1542	0.9091	−0.375	1124.40	870.00	−33.8	1.3747	0.0026
0.2382	0.9231	−0.545	1140.55	832.80	−46.2	1.3793	0.0035
0.3272	0.9373	−0.706	1157.21	796.70	−55.3	1.3835	0.0038
0.4218	0.9516	−0.831	1174.30	762.00	−60.5	1.3876	0.0039
0.5225	0.9660	−0.905	1190.76	730.10	−60.5	1.3915	0.0036
0.6299	0.9802	−0.918	1206.90	700.40	−55.8	1.3953	0.0032
0.7448	0.9938	−0.808	1221.64	674.20	−45.0	1.3990	0.0024

https://doi.org/10.1021/acs.jced.3c00344
J. Chem. Eng. Data 2024, 69, 1423−1447

Table 3. continued

x_1	ρ (g cm^{-3})	V^E (cm^3 mol^{-1})	c (m s^{-1})	κ_s (T Pa^{-1})	k_s^E(T Pa^{-1})	n_D	n_D^E
0.8678	1.0067	−0.553	1233.93	652.40	−27.1	1.4026	0.0014
1.0000	1.0174	0.000	1242.06	637.10	0.0	1.4059	0.0000
T = 313.15 K							
0.0000	0.8759	0.000	1072.35	992.82	0.0	1.3625	0.0000
0.0750	0.8896	−0.224	1086.25	952.70	−18.6	1.3679	0.0019
0.1542	0.9032	−0.408	1101.79	912.00	−35.3	1.3726	0.0029
0.2382	0.9172	−0.575	1118.09	872.20	−48.6	1.3773	0.0039
0.3272	0.9316	−0.752	1134.88	833.40	−58.3	1.3815	0.0042
0.4218	0.9460	−0.877	1152.29	796.10	−63.9	1.3857	0.0044
0.5225	0.9605	−0.966	1170.04	760.50	−65.1	1.3896	0.0041
0.6299	0.9749	−0.981	1186.40	728.80	−59.7	1.3933	0.0035
0.7448	0.9885	−0.868	1202.01	700.10	−48.4	1.3969	0.0027
0.8678	1.0012	−0.575	1214.67	677.00	−28.6	1.4004	0.0016
1.0000	1.0119	0.000	1224	659.62	0.0	1.4036	0.0000
T = 318.15 K							
0.0000	0.8697	0.000	1050.40	1042.18	0.0	1.3592	0.0000
0.0750	0.8835	−0.243	1064.90	998.10	−20.3	1.3649	0.0021
0.1542	0.8973	−0.442	1080.67	954.20	−37.9	1.3697	0.0031
0.2382	0.9114	−0.62	1097.90	910.20	−53.1	1.3746	0.0042
0.3272	0.9261	−0.819	1114.89	868.80	−63.0	1.3791	0.0047
0.4218	0.9405	−0.949	1132.65	828.80	−68.9	1.3834	0.0049
0.5225	0.9551	−1.035	1150.19	791.40	−69.4	1.3874	0.0046
0.6299	0.9694	−1.042	1166.70	757.80	−63.3	1.3913	0.0041
0.7448	0.9831	−0.913	1183.61	726.10	−52.3	1.3948	0.0030
0.8678	0.9957	−0.604	1196.41	701.60	−31.1	1.3981	0.0016
1.0000	1.0064	0.000	1205.38	683.91	0.0	1.4014	0.0000
T = 323.15 K							
0.0000	0.8633	0.000	1028.61	1094.75	0.0	1.3567	0.0000
0.0750	0.8774	−0.268	1043.59	1047.00	−22.6	1.3626	0.0023
0.1542	0.8913	−0.475	1059.56	999.30	−42.3	1.3677	0.0036
0.2382	0.9056	−0.668	1075.70	954.30	−56.5	1.3725	0.0045
0.3272	0.9203	−0.871	1092.80	909.90	−67.2	1.3772	0.0052
0.4218	0.9350	−1.014	1110.89	866.70	−73.7	1.3815	0.0054
0.5225	0.9496	−1.097	1128.73	826.60	−74.1	1.3855	0.0051
0.6299	0.9639	−1.094	1146.49	789.30	−68.5	1.3892	0.0044
0.7448	0.9776	−0.953	1162.86	756.50	−55.2	1.3927	0.0033
0.8678	0.9902	−0.636	1177.05	728.91	−33.3	1.3962	0.0020
1.0000	1.0008	0.000	1186.90	709.30	0.0	1.3991	0.0000

[a]Standard uncertainties u are $u(T)$ = 0.02 K and $u(p)$ = 0.04 MPa, and the combined expanded uncertainties Uc in mole fraction, density, speed of sound, refractive index, excess molar volume, excess isentropic compressibility, and excess refractive index are Uc(x) = 0.0005, Uc(ρ) = 0.0009 g cm^{-3}, Uc(c) = 2.91 m s^{-1}, Uc(n_D) = 0.0006, Uc(V^E) = 0.005 cm^3 mol^{-1}, Uc(k_s^E) = 0.2 T Pa^{-1}, and Uc(n_D^E) = 0.0009, respectively (0.95 level of confidence).

ities k_s^{id} were calculated by using the Benson and Kiyohara equation.[47,48]

$$k_s^{id} = \sum_{i=1}^{2} \phi_i[\kappa_{s,i} + TV_i(\alpha_i^2)/C_{p,i}] - \left\{T\left(\sum_{i=1}^{2} x_iV_i\right)\left(\sum_{i=1}^{2} \phi_i\alpha_i\right)^2 \Big/ \sum_{i=1}^{2} x_iC_{p,i}\right\} \quad (4)$$

Here, $C_{p,i}$, ϕ_i, and α_i are the molar heat capacity, volume fraction, and thermal expansion coefficient of the ith component, respectively. The $C_{p,i}$ values are taken from the literature.[49−52] The obtained k_s and k_s^E values are listed in Table 3.

However, the volume fraction and the thermal expansion coefficient were calculated from the following equations. The molar heat capacity and thermal expansion coefficient values are given in Table 4.

$$\phi_i = x_iV_i/\sum_{i=1}^{n} x_iV_i \quad (5)$$

$$\alpha_i = (\partial V/\partial T)_p/V = -1/\rho(\partial\rho^{-1}/\partial T)_p \quad (6)$$

The sign of excess isentropic compressibility (k_s^E) data provides vital information to understand the molecular interactions in liquid mixtures through hydrogen bonding, dipole−dipole, or dipole-induced dipole interactions, interstitial accommodation, and orientation ordering. The excess isentropic compressibility (k_s^E) data graphically depicted against the mole fraction (x_1) of EL with substituted ethanols or ethyl acetate at 298.15 K are shown in Figure 3.

A perusal of curves depicted in Figure 3 shows that a negative sign in k_s^E data was observed for all of the studied

https://doi.org/10.1021/acs.jced.3c00344
J. Chem. Eng. Data 2024, 69, 1423−1447

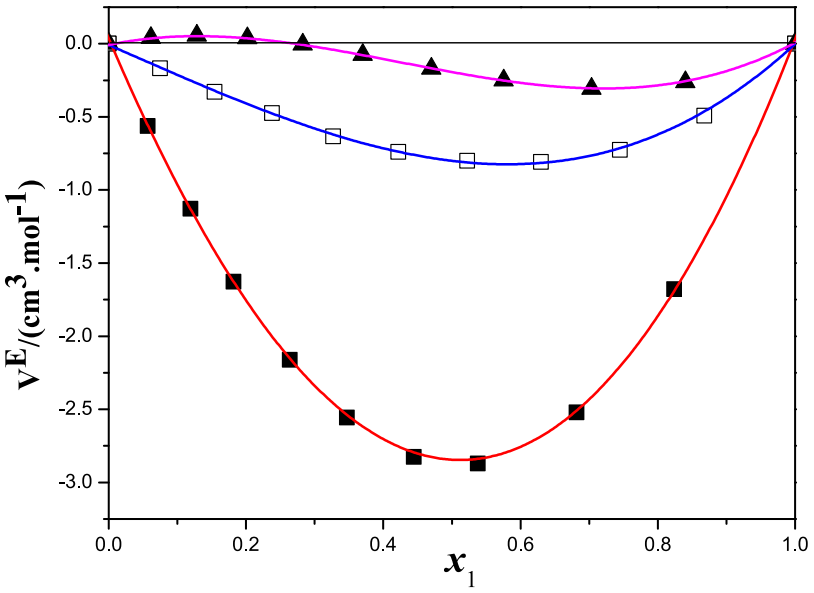

Figure 1. Plots of excess volume (V^E) vs mole fraction (x_1) of ethyl lactate with 2-aminoethanol (■), 2-chloroethanol (▲), and ethyl acetate (□) at 298.15 K.

binary systems. The negative k_s^E values indicate the presence of strong intermolecular interactions between component molecules through dipole-induced dipole interactions, hydrogen bonding formation, and interstitial accommodation between component molecules. The values of k_s^E can be set in the following order: EL + 2-AE > EL + EA > EL + 2-CE.

The quantity, excess refractive index (n_D^E), was calculated adopting the equation of Reis et al.,[53] which is given below

$$n_D^E = n_D - [\varphi_1^2 n_{D1} + \varphi_2^2 n_{D2}]^{1/2} \quad (7)$$

where, φ_1, φ_2, n_{D1}, and n_{D2} are the volume fractions and refractive indices of components 1 and 2, respectively, and n_D is the refractive index of the mixture.

The results of excess refractive index (n_D^E) for three binary systems (EL + 2-AE or 2-CE or EA) at 298.15 K are graphically represented in Figure 4. The n_D^E values are negative for EL + 2-CE and positive for EL + 2-AE or EA. This behavior can be explained by considering that when the packing effect decreases, the number of dipoles per unit volume diminishes and therefore n_D^E also becomes smaller, giving rise to negative n_D^E.

The values of V^E, k_s^E, and n_D^E were related to the mole fraction of binary mixtures, correlated by the Redlich−Kister equation.[54]

$$y^E = x_1 x_2 \sum_{i=0}^{n} a_1 (x_1 - x_2)^i \quad (8)$$

where y^E is V^E or k_s^E or n_D^E, while x_1 and x_2 are the mole fractions of pure components.

The corresponding standard deviations (σ) were defined as

$$\sigma = \left[\sum_{i=1}^{n} (y_{exp}^E - y_{clac}^E)^2 / n - p \right]^{1/2} \quad (9)$$

Here, y_{calc}^E represents the calculated values of V^E or k_s^E or n_D^E. n and p denote the number of data points and coefficients in eq 8 and the correlated results are listed in Table 5.

3.2. FT-IR Studies. Figures S2−S4 show the FT-IR spectrum of binary liquid mixtures of EL with substituted ethanols or ethyl acetate at different mole fractions within the range of 500−4000 cm$^-$; these values are reported in Table 6.

From the spectrum, it is very important to examine the −C═O, $-NH_2$, −C−Cl, and −OH stretching bands to predict the possible intra- and intermolecular interactions in binary systems. A broad band appears at 3451 $cm^{-1}$of pure EL, as shown in Figure S3, which indicates the presence of intermolecular hydrogen bonding between the like molecules, and a sharp band appears at 1729 cm^{-1}, which is assigned to the −C═O stretching vibrational frequency of pure EL. Additionally, a strong band observed at 2856 cm^{-1} for 2-AE is assigned to $-NH_2$ stretching. When 2-AE was mixed with EL incrementally, the stretching vibrational frequency of the −OH group in EL was found to shift toward a lower wavenumber from 3451 to 3288 cm^{-1} and the $-NH_2$ group of the 2-AE stretching vibrational frequency was increased from 2856 to 2872 cm^{-1}. This observation is attributed vividly to the rupturing of intermolecular hydrogen bonds in pure EL molecules and a stronger hydrogen bond (N−H···O−H) between the hydrogen atom of the $-NH_2$ group of 2-AE and the oxygen atom of the −OH group in the EL molecule. Furthermore, the shape of −C═O stretching bands changed significantly from 1729 to 1647 cm^{-1}. It can be concluded that a new hydrogen bond (N−H···O═C−) formed between the oxygen atom in −C═O of EL and the hydrogen atom of $-NH_2$ in 2-AE.

Moreover, Figure S4 illustrates the FT-IR spectrum of pure 2-CE and EL at different mole fractions (x_1 = 0.3, 0.5, and 0.7) for the binary system of EL + 2-CE within the range of 4000−400 cm^{-1}. Herein, a broad band appears at 3340 cm^{-1}, which indicates the −OH stretching vibrational frequency of pure 2-CE. On the addition of EL to 2-CE, the absorption intensity of the broad −OH stretching band of 2-CE was shifted to 3348, 3375, and 3432 cm^{-1} for the binary liquid mixtures of EL with 2-CE at x_1 = 0.3, 0.5, and 0.7, respectively. Also, as shown in Figure S4, a sharp band appears at 1729 cm^{-1}, which is assigned to the −C═O stretching vibrational frequency of

https://doi.org/10.1021/acs.jced.3c00344
J. Chem. Eng. Data 2024, 69, 1423−1447

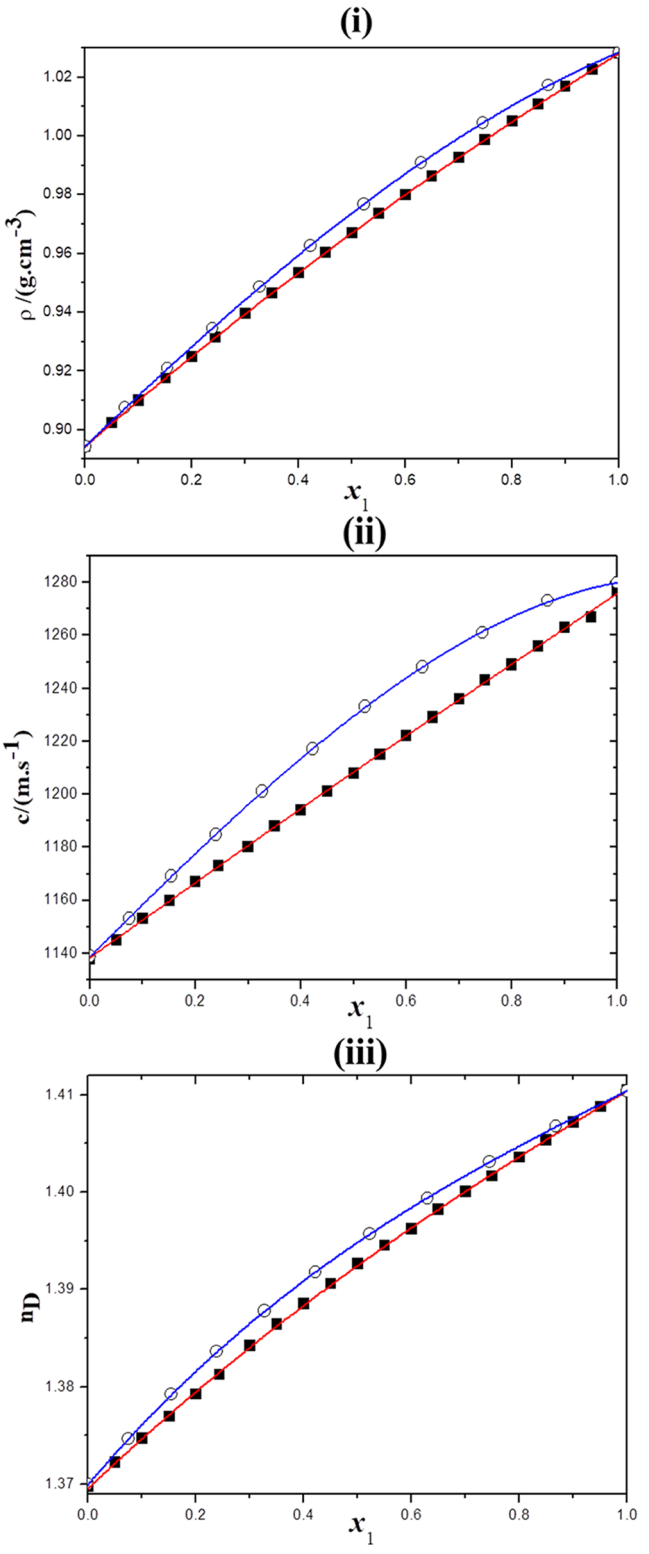

Figure 2. Variations of the experimental (i) density (ρ), (ii) speed of sound (c), and (iii) refractive index (n_D) data for binary systems of EL + EA at 298.15 K; (o) this work and (■) ref 22.

pure EL. On the addition of EL to 2-CE, the −C═O stretching vibrational frequency shifted to 1736, 1732, and 1730 cm^{-1} for the binary liquid mixtures of EL with 2-CE at x_1 = 0.3, 0.5, and 0.7, respectively. This behavior can explain the formation of the intermolecular hydrogen bond (−C═O···H−O−) between the hydrogen atom of the −OH group in the 2-CE molecule and the carbonyl group of EL.

Table 4. Molar Heat Capacity ($C_{p,i}$) Values Taken from the Available Literature[49−52] and the Thermal Expansion Coefficient (α_i) Calculated from Eq 6 for the Pure Liquid Components at T = 298.15−323.15 K and at Pressure p = 0.1 MPa

T/K	ethyl lactate	2-chloroethanol	2-aminoethanol	ethyl acetate
		$C_{p,i}$ (J mol^{-1} K^{-1})		
298.15	258.62[49]	129.53[50]	161.89[50]	169.9[51]
303.15	269.42[49]	131.6[50]	164.6[50]	171[52]
308.15	271.75[49]	133.8[50]	167.8[50]	172.95[52]
313.15	274.13[49]	136[50]	171[50]	174.12[52]
318.15	276.54[49]	138.2[50]	176.58[50]	177.77[52]
323.15	279.92[49]	140[50]	179.32[50]	178.2[52]
		α_i (k K^{-1})		
298.15	1.0606	0.7119	0.837	1.3622
303.15	1.0634	0.8637	0.7919	1.38
308.15	1.0843	0.9695	0.7997	1.3946
313.15	1.0892	1.418	0.6945	1.4209
318.15	1.106	0.8007	0.9287	1.4374
323.15	1.1141	0.5776	0.7694	1.4629

3.3. Results about Property Modeling. The pure-component parameters required in the equation of state were optimized using the objective function defined by eq 10

$$\mathrm{OF} = \sum_{i=1}^{n_p} \left(\frac{P_i^{\mathrm{calc.}} - P_i^{\mathrm{exp.}}}{P_i^{\mathrm{exp.}}} \right)^2 + \left(\frac{\rho_i^{\mathrm{calc.}} - \rho_i^{\mathrm{exp.}}}{\rho_i^{\mathrm{exp.}}} \right)^2 \quad (10)$$

where n_p is the number of experimental points, ρ is the liquid density, P is the vapor pressure, calc. is related to the calculated value using PC-SAFT EoS, and exp. is related to the experimental value. The experimental liquid density data obtained in this work and the vapor pressure data published by DIPPR[55] were used in eq 10. Also, Figure 5 reveals that the theoretical models in this work evidently represent the density for the ethyl lactate + 2-aminoethanol binary system.

The absolute average deviation for density, speed of sound, and refractive index can be calculated from eq 11

$$\%\mathrm{AAD}\xi = \frac{100}{n_p} \sum_{i=1}^{n} \frac{|\xi_i^{\mathrm{exp.}} - \xi_i^{\mathrm{calc.}}|}{\xi_i^{\mathrm{exp.}}} \quad (11)$$

where ξ is the density or speed of sound or refractive index. Table 7 shows the parameters for the pure fluids. Deviations in vapor pressure and liquid density are also observed. According to these values, PC-SAFT correctly adjusts the vapor pressure and liquid density of the fluids.

Table 8 shows the adjustable binary parameters in the PC-SAFT modeling for the density of binary mixtures. The deviation in the density and speed of sound is also included in this table. From Table 8, we can see that PC-SAFT EoS correctly correlates the experimental density of the mixtures (overall deviation = 0.09%), while the prediction for the speed of sound with NR and PC-SAFT EoS is very good for EL + CE and EL + EA mixtures (overall deviation = 0.15 and 0.71%, respectively).

Moreover, in this work, Figure 6 depicts the PC-SAFT EoS model, which evidently represents the speed of sound for the ethyl lactate + 2-chloroethanol binary mixture.

https://doi.org/10.1021/acs.jced.3c00344
J. Chem. Eng. Data 2024, 69, 1423−1447

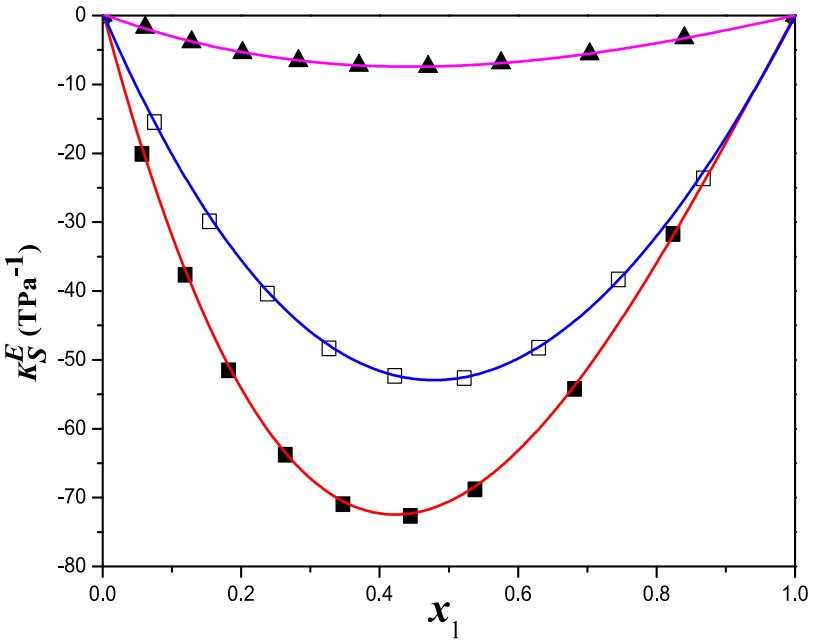

Figure 3. Curves of excess isentropic compressibility (k_s^E) against the mole fraction (x_1) of EL at 298.15 K for three binary systems: EL + 2-AE (■), EL + 2-CE (▲), and EL + EA (□).

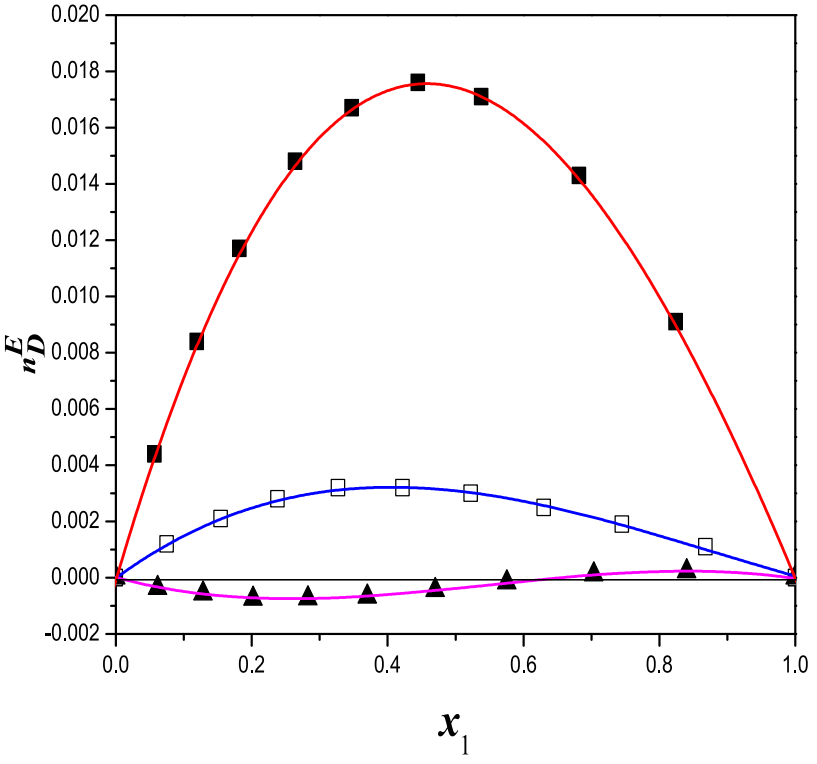

Figure 4. Curves of excess refractive index (n_D^E) against the mole fraction (x_1) of ethyl lactate with 2-aminoethanol (■), 2-chloroethanol (▲), and ethyl acetate (□) at 298.15 K.

Finally, Table 9 summarizes the deviations in the refractive index using four mixing rules. According to these values, it is concluded that the four mixing rules combined with PC-SAFT present results that are in agreement with the experimental data; however, the Lorentz−Lorenz rule was the best option (overall deviation = 0.04%).

On the other hand, from Figure 7, it can be seen that the Lorentz−Lorenz mixing rule correctly predicts the dependence of the refractive index with the mole fraction of ethyl lactate and the temperature for the ethyl lactate + ethyl acetate mixture.

3.4. Computational Results. *3.4.1. Hydrogen Bonding Interactions: Interacting Atoms and Stabilization Energy.* According to the theoretical calculations, the intermolecular hydrogen bonding interactions with different interacting centers with varied stabilization energies are shown in Table

https://doi.org/10.1021/acs.jced.3c00344
J. Chem. Eng. Data 2024, 69, 1423−1447

Table 5. Redlich−Kister Fitting Parameters and Root-Mean-Square Deviation, σ, for the Binary Mixtures at T = 298.15, 303.15, 308.15, 313.15, 318.15, and 323.15 K[a]

	A_i	298.15 K	303.15 K	308.15 K	313.15 K	318.15 K	323.15 K
{Ethyl Lactate (x_1) + 2-Aminoethanol (x_2)}							
V^E (cm^3 mol^{-1})	A_0	−11.527	−11.954	−12.406	−12.867	−13.346	−13.843
	A_1	−0.515	−0.653	−0.805	−0.973	−1.149	−1.354
	A_2	0.641	0.596	0.571	0.533	0.493	0.445
	σ	0.002	0.001	0.002	0.001	0.001	0.001
k_s^E (T Pa^{-1})	A_0	−283.860	−323.561	−354.170	−380.565	−419.838	−457.384
	A_1	97.187	106.315	108.230	112.905	109.664	115.956
	A_2	0.143	−1.830	−6.048	−29.224	−18.317	−12.888
	σ	0.219	0.314	0.221	0.638	0.312	0.305
n_D^E	A_0	0.044	0.045	0.047	0.049	0.050	0.052
	A_1	−0.004	−0.003	−0.003	−0.004	−0.003	−0.003
	A_2	0.000	0.000	0.000	−0.001	0.000	−0.001
	σ	0.000	0.000	0.000	0.000	0.000	0.000
{Ethyl Lactate (x_1) + 2-Chloroethanol (x_2)}							
V^E (cm^3 mol^{-1})	A_0	−0.708	−0.797	−0.912	−1.001	−1.065	−1.144
	A_1	−1.738	−1.655	−1.590	−1.514	−1.471	−1.460
	A_2	−0.018	−0.064	−0.035	−0.056	−0.054	−0.062
	σ	0.001	0.002	0.002	0.002	0.002	0.002
k_s^E (T Pa^{-1})	A_0	−29.594	−37.847	−45.903	−55.752	−64.580	−74.506
	A_1	6.788	9.551	9.037	11.003	15.697	20.551
	A_2	1.179	−2.337	−3.213	−2.580	−4.657	−2.264
	σ	0.109	0.078	0.060	0.073	0.100	0.099
n_D^E	A_0	−0.017	−0.016	−0.015	−0.014	−0.013	−0.012
	A_1	0.009	0.009	0.008	0.008	0.008	0.007
	A_2	−0.001	0.000	0.001	0.001	0.001	0.001
	σ	0.000	0.000	0.000	0.000	0.000	0.000
{Ethyl Lactate (x_1) + Ethyl Acetate (x_2)}							
V^E (cm^3 mol^{-1})	A_0	−3.185	−3.358	−3.580	−3.809	−4.091	−4.331
	A_1	−1.155	−1.200	−1.268	−1.335	−1.305	−1.277
	A_2	−0.349	−0.532	−0.445	−0.497	−0.420	−0.457
	σ	0.008	0.009	0.006	0.008	0.009	0.010
k_s^E (T Pa^{-1})	A_0	−211.678	−227.474	−244.147	−260.654	−278.965	−297.754
	A_1	18.308	13.952	17.001	13.682	16.674	21.272
	A_2	−6.334	−10.249	−4.458	1.433	−7.284	−16.026
	σ	0.349	0.242	0.265	0.185	0.458	0.291
n_D^E	A_0	0.019	0.020	0.021	0.023	0.025	0.027
	A_1	−0.006	−0.006	−0.006	−0.007	−0.008	−0.008
	A_2	0.001	0.002	0.004	0.004	0.002	0.004
	σ	0.000	0.000	0.000	0.000	0.000	0.000

[a]Standard uncertainties u are $u(T)$ = 0.02 K and $u(p)$ = 0.04 MPa, and the combined expanded uncertainties Uc in mole fraction, density, speed of sound, refractive index, excess molar volume, excess isentropic compressibility, and excess refractive index are Uc(x) = 0.0005, Uc(ρ) = 0.0009 g cm^{-3}, Uc(c) = 2.91 m s^{-1}, Uc(n_D) = 0.0006, Uc(V^E) = 0.005 cm^3 mol^{-1}, Uc(k_s^E) = 0.2 T Pa^{-1}, and Uc(n_D^E) = 0.0009, respectively (0.95 level of confidence).

10 for three binary systems of ethyl lactate (EL) with 2-aminoethanol (a), ethyl lactate with 2-chloroethanol (b), and ethyl lactate with ethyl acetate (c). The calculations were performed using the ADF 2020.102 package at the BP86-D3 (BJ) level with the TZP basis set, and the SCF convergence criteria has been maintained the same as those of the geometry optimizations above.

Moreover, the optimized geometries of ethyl lactate, 2-aminoethanol, 2-chloroethanol, and ethyl acetate were calculated at the BP86 level of theory with the TZP basis set with the empirical dispersion GD3BJ and are represented in Figure 8.

Hydrogen Bonding Interactions (Interactions Across Same Molecular Species). The molecules are found to show multiple intermolecular hydrogen bonding interactions with different interacting centers with varied stabilization energies. The optimized structures are shown in Table 11.

Interacting Set (a): Ethyl Lactate with 2-Aminoethanol. In this set, from theoretical calculations, three possible interactions are found having the largest stabilization interaction. The bond length of the O−H bond was elongated with an increased stabilization energy as well as the distance of the hydrogen bonding interaction, which is in direct relation with the stabilization energy.

Interacting Set (b): Ethyl Lactate with 2-Chloroethanol. The three stabilized interactions are found, with all having very similar stabilization energies. The OH···Cl interactions are comparably stronger as of OH···O hydrogen bonds. The elongation of the OH (hydroxyl group) bond was observed showing deviations ranging from 0.1 to 0.15 Å with the

https://doi.org/10.1021/acs.jced.3c00344
J. Chem. Eng. Data 2024, 69, 1423−1447

Table 6. Experimental Neat FT-IR Stretching Wavenumbers (cm^{-1}) of Distinct Functional Groups of Pure Liquids and the Mixtures of EL + Substituted Ethanols or Ethyl Acetate

mole fraction	−OH (cm^{-1})	−C═O (cm^{-1})	−Cl (cm^{-1})	$-NH_2$ (cm^{-1})
EL + 2-AE				
0.0	3172			2856
0.3	3288			2859
0.5	3293	1647		2872
0.7	3383	1731		
1	3451	1729		
EL + 2-CE				
0.0	3340		658	
0.3	3348	1736	659	
0.5	3375	1732	660	
0.7	3432	1730		
1	3451	1729		
EL + EA				
0.0		1736		
0.3	3495	1735		
0.5	3470	1735		
0.7	3462	1733		
1	3451	1729		

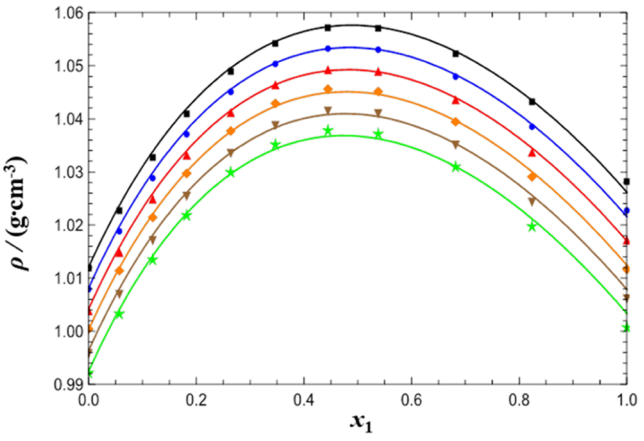

Figure 5. Experimental density and calculated density using PC-SAFT EoS for the ethyl lactate (1) + 2-aminoethanol (2) mixture. Symbols refer to experimental data at temperatures (■) 298.15 K, (blue circle solid) 303.15 K, (red triangle up solid) 308.15 K, (orange tilted square solid) 313.15 K, (olive green triangle down solid) 318.15 K, and (green star solid) 323.15 K; solid lines represent the theoretical data obtained with PC-SAFT.

nonhydrogen-bonded optimized chloroethanol structure, showing an OH bond length of 0.976 Å. The bond lengths of OH in the above four interactions are directly related to the corresponding stabilization energy. The hydrogen bond length also follows the similar trend.

Table 8. Fitted Binary Interaction Parameters and the Absolute Average Deviation for the Density and Speed of Sound of All of the Mixtures

mixture	k_{ij}	%AADρ	%AADu
ethyl lactate (1) + 2-aminoethanol (2)	−0.0552	0.05	2.77
ethyl lactate (1) + 2-chloroethanol (2)	0.0354	0.11	0.15
ethyl lactate (1) + ethyl acetate (2)	0.0160	0.12	0.71
	overall	0.09	1.21

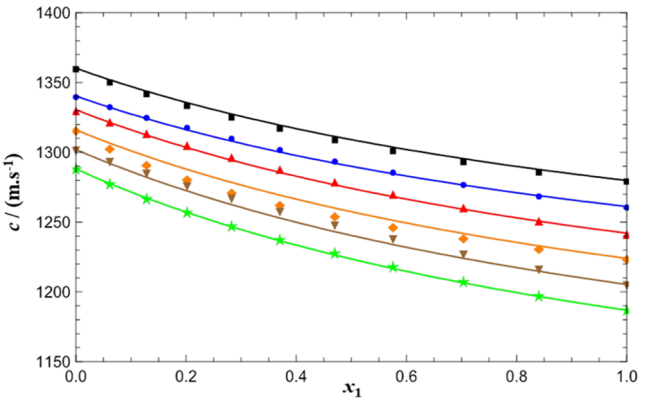

Figure 6. Experimental speed of sound and calculated speed of sound using PC-SAFT EoS + NR for the ethyl lactate (1) + 2-chloroethanol (2) mixture. Symbols refer to experimental data at temperatures (■) 298.15 K, (blue circle solid) 303.15 K, (red triangle up solid) 308.15 K, (orange tilted square solid) 313.15 K, (olive green triangle down solid) 318.15 K, and (green star solid) 323.15 K; solid lines represent the theoretical data obtained with PC-SAFT + NR.

Table 9. Absolute Average Deviation for Refractive Index (%AADn_D) Using Four Mixing Rules and PC-SAFT EoS for All of the Mixtures

mixture	LL	GD	LP	EK
ethyl lactate (1) + 2-aminoethanol (2)	0.05	0.12	0.21	0.08
ethyl lactate (1) + 2-chloroethanol (2)	0.03	0.03	0.03	0.03
ethyl lactate (1) + ethyl acetate (2)	0.04	0.05	0.06	0.04
overall	0.04	0.07	0.10	0.05

Interacting Set (c): Ethyl Lactate with Ethyl Acetate. Only one possible interaction was observed for this set, possibly due to the increased steric hindrance compared to the former sets of molecules. The elongation of the OH (hydroxyl group) bond was observed, which deviated from the nonhydrogen-bonded structure by 0.12 Å.

3.4.2. QTAIM Analysis. To get deeper insights into the nature of bonding interactions between the molecules, topological analysis has been carried out for analyzing the electron density $\rho(r)$ using Bader's quantum theory of atoms in molecules (AIM). Furthermore, the contour plots of Laplacian

Table 7. Parameters for the Pure Components Required in PC-SAFT EoS and the Absolute Average Deviation for Vapor Pressure and Liquid Density (the Temperature Range was 298.15−323.15 K)

fluid	m	σ/(Å)	ε/k_B/(K)	ε^{AB}/k_B/(K)	k^{AB}	%AADP	%AADρ
ethyl lactate	2.000	4.3610	394.17	643.71	0.0095	0.16	0.14
2-aminoethanol	3.650	2.8698	232.81	1537.18	0.1023	0.01	0.02
2-chloroethanol	2.950	3.1626	307.54	821.42	0.0145	0.17	0.08
ethyl acetate	3.650	3.2506	227.27	0	0	0.04	0.06
		overall				0.10	0.08

https://doi.org/10.1021/acs.jced.3c00344
J. Chem. Eng. Data 2024, 69, 1423−1447

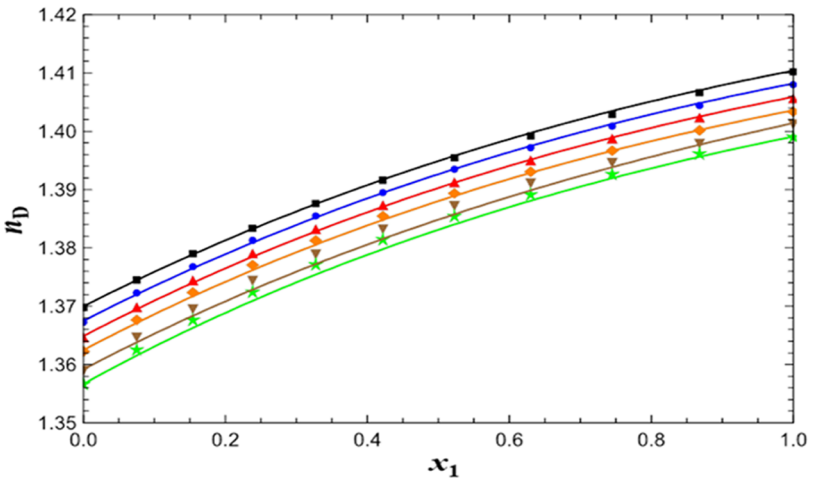

Figure 7. Experimental refractive indices and calculated refractive indices using PC-SAFT EoS + the Lorentz−Lorenz mixing rule for the ethyl lactate (1) + ethyl acetate (2) mixture. Symbols refer to experimental data at temperatures (■) 298.15 K, (blue circle solid) 303.15 K, (red triangle up solid) 308.15 K, (orange tilted square solid) 313.15 K, (olive green triangle down solid) 318.15 K, and (green star solid) 323.15 K; solid lines represent the theoretical data obtained with PC-SAFT + the Lorentz−Lorenz mixing rule.

distributions for the ethyl lactate (EL) + 2-aminoethanol binary system are represented in Figure 9.

Interacting Set (a): Ethyl Lactate with 2-Aminoethanol. The microscopic characteristics of the materials, such as interatomic interactions, ultimately govern their macroscopic behavior.[56] The presence of a bond critical point (BCP)[57,58] is a need for the creation of a chemical bond. The chemical bonds can be quantified in terms of characteristics of the BCPs in electron density, according to Bader's quantum theory of atoms in molecules (QTAIM). Information on the type of atomic interactions is obtained through an analysis of the electron density parameters at BCPs. However, the electron density map $\rho(r)$ and the Laplacian of electron density contour plots are graphically shown in Figure 10 for the ethyl lactate + 2-chloroethanol binary system.

Interacting Set (b): Ethyl Lactate with 2-Chloroethanol. The distinction between noncovalent closed-shell interactions (ionic, etc.) and covalent ones is made using difference or deformation electron densities as well as the Laplacian of electron density at the BCP, which describes the concentration of electron density in the bonding region. But these traits are insufficient to recognize weak covalent bonds.[59] Likewise, the contour plot of the Laplacian distribution $[\nabla^2 \rho(r)]$ in the O7−H9−O13 plane is depicted in Figure 11 for the ethyl lactate + ethyl acetate interacting set. The electron density exits the internuclear area when such bonds are established, but the remaining density is sufficient for covalent bonding to develop since the potential energy[60] absolute value (magnitude) increases. The energy density H is therefore employed in addition to the Laplacian (∇^2) and the deformation density. $H = G + V$, where G and V, respectively, stand for the kinetic and potential energy densities at the BCP. While the bond has a covalent component at $H < 0$ (rho is stabilizing), the condition $H > 0$ (rho is destabilizing) corresponds to the noncovalent closed-shell contact. Therefore, the preponderance of local potential energy at the BCP describes the covalent bond. Therefore, a chemical bond must be described energetically and electrostatically (Hellmann−Feynman).[61]

Interacting Set (C): Ethyl Lactate with Ethyl Acetate. The three types of atomic interactions are closed-shell interactions, shared interactions, and transit (intermediate) interactions. Covalent and polar covalent bonds are examples of shared interactions. Partially covalent contacts, such as metallic bonds, strong hydrogen bonds, coordination (dative) bonds, etc., are examples of intermediate interactions. Ionic bonds and weak intermolecular contacts (weak and medium hydrogen bonds, van der Waals interactions, etc.) are examples of closed-shell interactions. For the record, covalent bonds are what characterize the strongest hydrogen and coordination bonds.

Additionally, the bond degree parameter BD = H/rho (the total energy per electron at the BCP) can be used to categorize atomic interactions. The BD parameter is positive and indicates a strengthening degree (SD) for noncovalent closed-shell interactions, the amount of the SD increases with the interaction's strength and degree of closure. The covalence degree (CD) of shared and intermediate (partially covalent) contacts is indicated by the negative BD parameter; the stronger and more covalent the connections, the larger are the CD magnitudes.

In this work, AIM analysis was performed for a, b, and c to get more insight into the nature of hydrogen bonding interactions. Moreover, QTAIM analysis was performed for three binary systems to get more insight into the nature of hydrogen bonding interactions. Also, the interacting hydrogen bonds are given in Table 12.

The topological analysis of set a shows that the electron density $\rho(r)$ at the H19−N9 bond critical point (BCP) is 0.045 a.u, whose value is small, indicating a shared-type interaction. This was further confirmed by the positive Laplacian of the electron density value, which is close to zero, at the BCP between the H19−N9 bond, and the position of the BCP is close to maximum. The value of η, which is 0.35, indicates the closed-type interaction across this hydrogen bond. This nature of the closed shared-type interaction is further confirmed by the negative value of $H(r)$, which is −0.01. The ellipticity value of 0.007 indicates that the nature of bonding is more of a sigma-type interaction. In conclusion, all of the parameters mentioned above confirm that the nature of bonding across H19−N9 is a closed shared type of interaction.

This was followed by the topological analysis of set b, which shows that the electron density ρ(r) at the H25−O5 bond critical point (BCP) is 0.024 a.u, whose value is small,

https://doi.org/10.1021/acs.jced.3c00344
J. Chem. Eng. Data 2024, 69, 1423−1447

Table 10. Representation of Interacting Sets {a, b, c} with Their Variations in the Atomic Interacting Centers Along with Bond Lengths in Angstroms (Å) and Stabilization Energy

Interacting set (a): Ethyl Lactate with 2-Amino ethanol	Stabilization energy (Kcal/mol)
1. 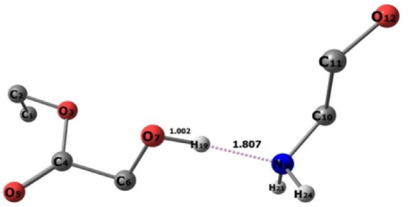	**10.89**
2. 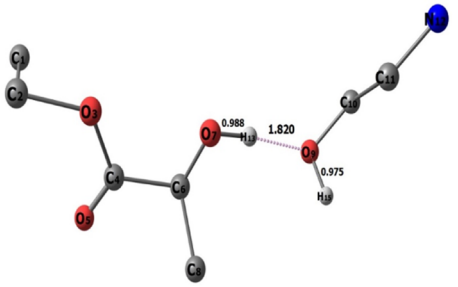	**5.04**
3. 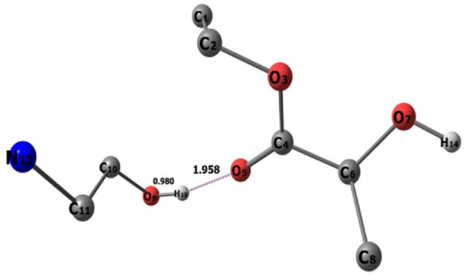	**4.32**
Interacting set (b): Ethyl lactate with 2-Chloro ethanol	
4. 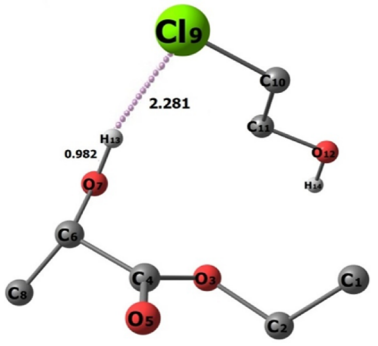	**5.02**
5. 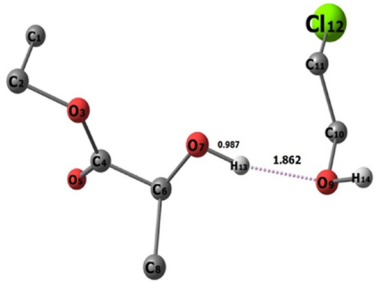	**4.84**

https://doi.org/10.1021/acs.jced.3c00344
J. Chem. Eng. Data 2024, 69, 1423−1447

Table 10. continued

6. 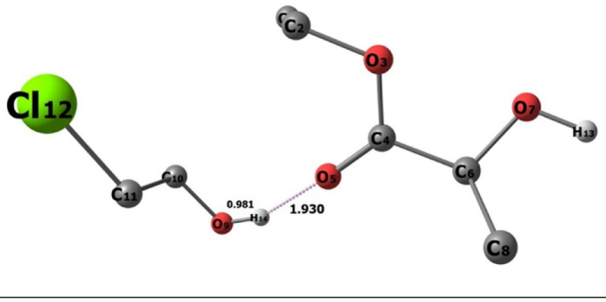	6.01
Interacting set (C): Ethyl lactate with Ethyl acetate	
7. 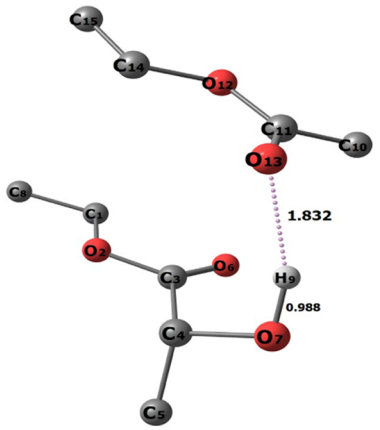	7.12

indicating a shared-type interaction. This was further confirmed by the positive Laplacian of the electron density value, which is close to zero, at the BCP between the H25−O5 bond, and the position of the BCP is close to maximum. The value of η, which is 0.23, indicates the closed type of interaction across this hydrogen bond similar to the set a interaction. This nature of a closed shared-type interaction is further confirmed by the negative value of $H(r)$, which is −0.0002. The ellipticity value of 0.057 indicates that the nature of bonding is more of a sigma-type interaction and seems to have more pi character compared to the set a interaction, as given in the table above. In conclusion, all of the parameters mentioned above confirm that the nature of bonding across H25−O5 is a closed shared type of interaction. The set c QTAIM analysis also infers the presence of a closed-shell-type interaction as of the previous two sets a and b. In conclusion, QTAIM analysis predicts the nature of the bonding interactions across the hydrogen bonds in the binary solutions. The most stabilized hydrogen bonding interaction was chosen, which is believed to be dominant at RT conditions. From the analysis, the nature of bonding is found to be weaker and a closed-shell shared-type interaction in all of the cases a−c.

3.4.3. Noncovalent Interaction Index Analysis. According to the divergence theorem,[62] the sign of the density's Laplacian ($\nabla^2\rho$) determines whether the net gradient flow of density is entering ($\nabla^2\rho < 0$) or leaving ($\nabla^2\rho > 0$) an infinitesimal volume surrounding a reference point. The hydrogen bond interactions between selected cross-associated complexes (a, b, and c) are represented in Figure 12.

As a result, the sign of $\nabla^2\rho$ determines if the density at that site is depleted or concentrated in comparison to the surroundings. The Laplacian sign cannot be used to discriminate between various weak interaction types since it is largely contributed by nuclei (negative).[63] Instead, contributions to the Laplacian along its greatest variation axis must be investigated. These contributions are of the electron-density Hessian [$\nabla^2\rho = \lambda_1 + \lambda_2 + \lambda_3$, ($\lambda_1 < \lambda_2 < \lambda_3$)] matrix eigenvalues λ_i. All of the eigenvalues near the nuclei are negative, but $\lambda_3 > 0$ distant from them. The values of λ_3 change in molecules in the internuclear direction, whereas the values of λ_1 and λ_2 describe the change in density in the plane normal to the eigenvector of λ_3.

Curiously, the subsequent eigenvalue (λ_2) can be either certain or negative, contingent upon the association type. One thing that distinguishes bonding-type interactions, for example, hydrogen bonds, is an accumulation of electron density perpendicular to the bond and $\lambda_2 < 0$. Density depletion occurs when $\lambda_2 > 0$ occurs as a result of nonbonded interactions like steric repulsion. Last but not the least, van der Waals interactions have a density overlap that is so small that it gives $\lambda_2 \lesssim 0$. As a result, we are able to identify various kinds of weak interactions through analysis of the sign of λ_2, whereas we are able to evaluate the interaction's strength through the density itself. The interacting sets a−c below demonstrate the dependence of $s(r)$ on sign (λ_2)ρ. Figures

https://doi.org/10.1021/acs.jced.3c00344
J. Chem. Eng. Data 2024, 69, 1423−1447

(i) Ethyl Lactate:

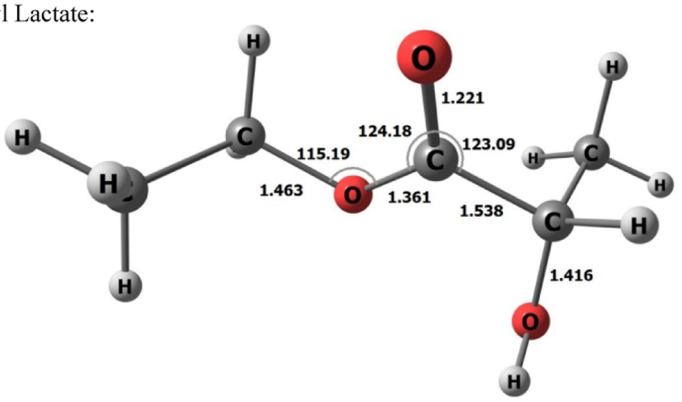

(ii) 2-Amino Ethanol:

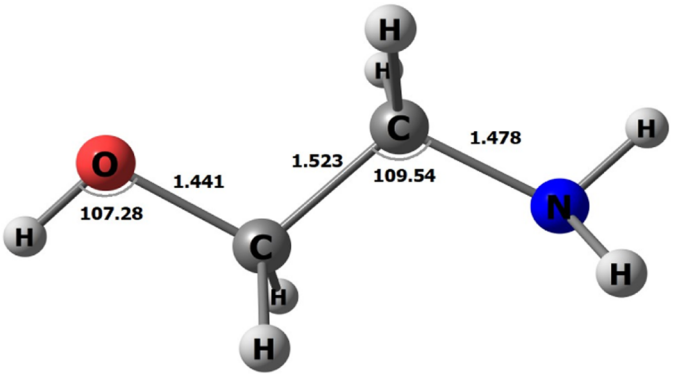

(iii) 2-Chloro ethanol:

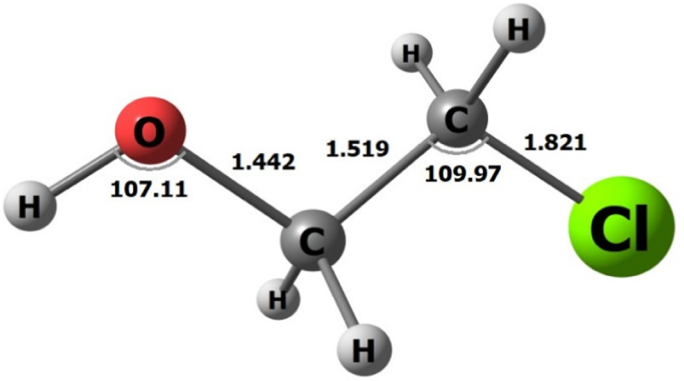

(iv) Ethyl acetate:

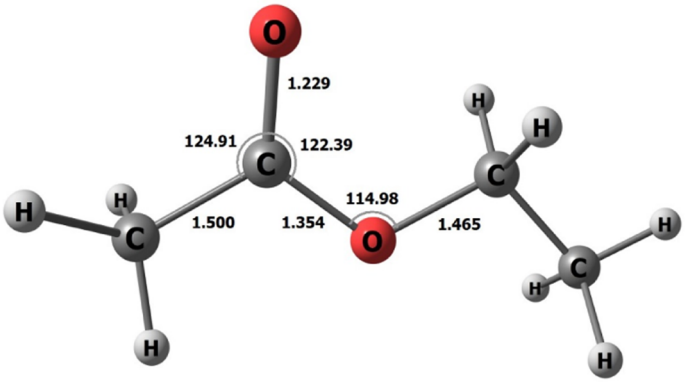

Figure 8. Optimized geometries of (i) ethyl lactate, (ii) 2-aminoethanol, (iii) 2-chloroethanol, and (iv) ethyl acetate calculated at the BP86 level of theory with the TZP basis set with the empirical dispersion GD3BJ. The corresponding bond lengths and bond angles are in angstroms (Å) and degrees (deg), respectively.

https://doi.org/10.1021/acs.jced.3c00344
J. Chem. Eng. Data 2024, 69, 1423−1447

Table 11. Interacting Dimers with their Variations in the Atomic Interacting Centers Along with Bond Lengths in Angstroms (Å)[a]

Ethyl Lactate	Stabilization energy (Kcal/mol)
1. 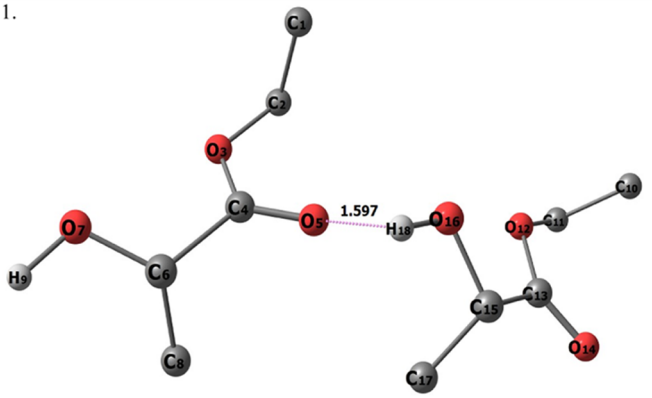	2.72
2. 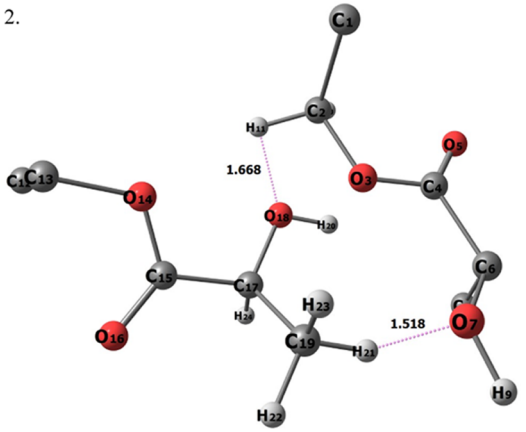	2.25
3. 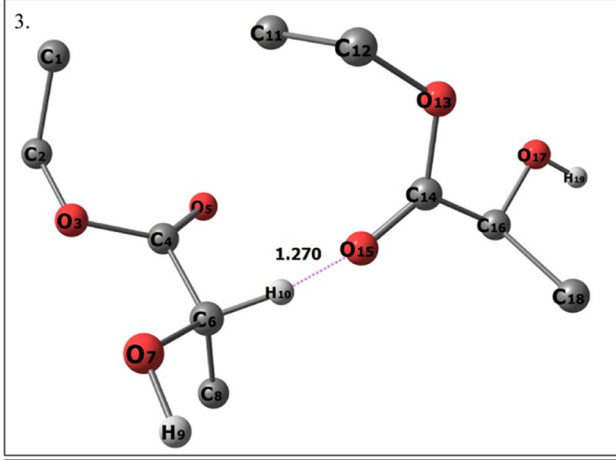	3.78
2-Chloro ethanol	Stabilization energy (Kcal/mol)
1. 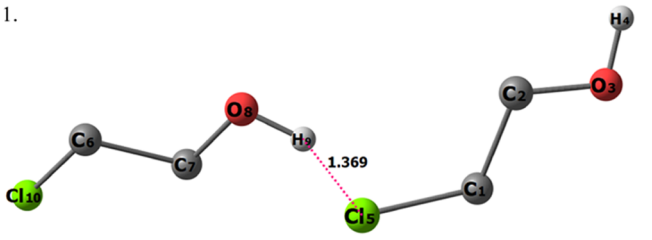	5.77

https://doi.org/10.1021/acs.jced.3c00344
J. Chem. Eng. Data 2024, 69, 1423−1447

Table 11. continued

2. 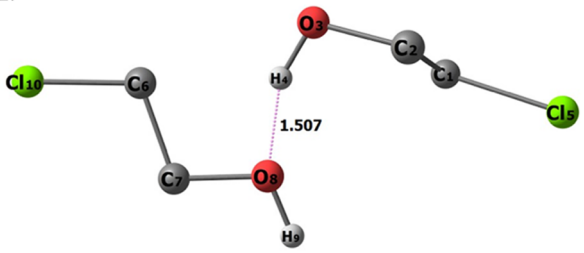	7.91
Ethyl acetate	Stabilization energy (Kcal/mol)
1. 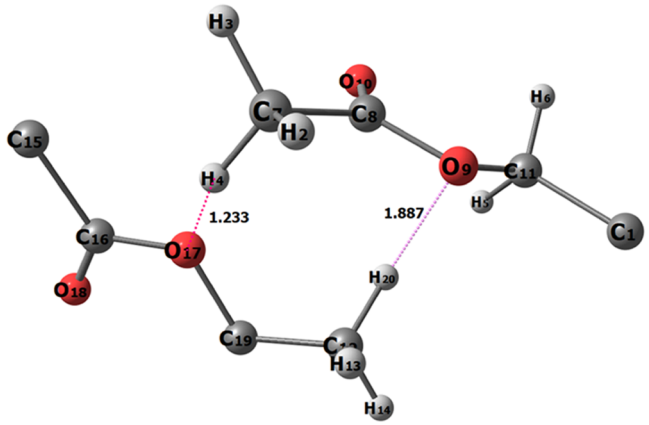	5.63
2. 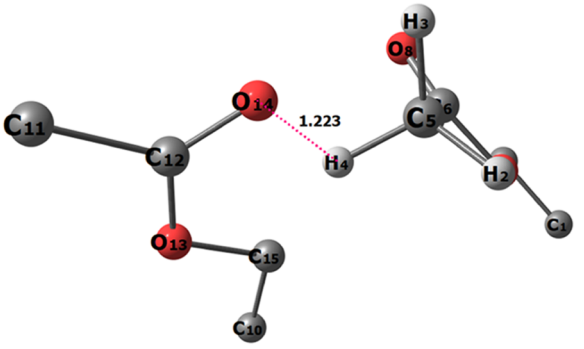	4.01
2-Amino Ethanol	Stabilization energy (Kcal/mol)
1. 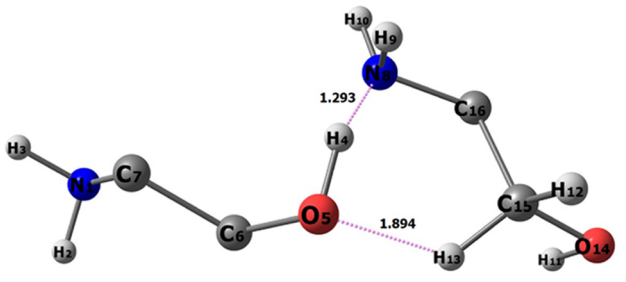	15.67

https://doi.org/10.1021/acs.jced.3c00344
J. Chem. Eng. Data 2024, 69, 1423−1447

Table 11. continued

2. 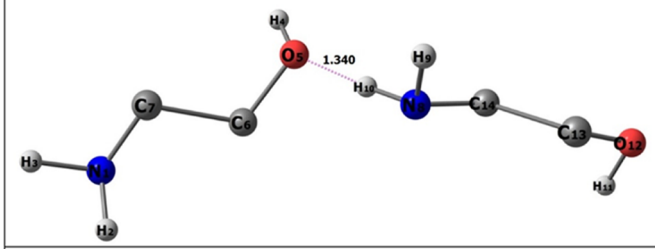	4.78
3. 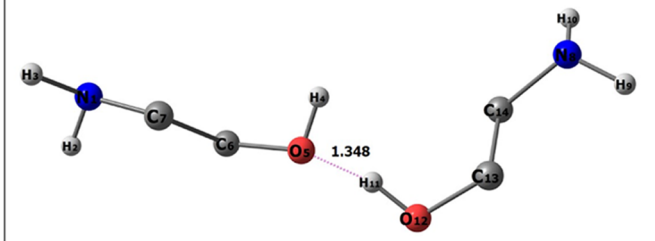	7.57
4. 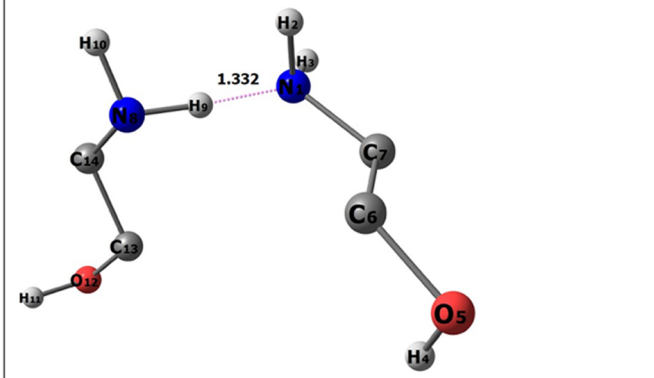	6.21

[a]A few hydrogen atoms are omitted for clarity. The stabilization energy represented above in the table is the energy difference between individual molecules without interaction and molecules with interaction. The molecules that are involved in intermolecular hydrogen bonding are found to have a lower energy than individual separate molecules

Table 12. QTAIM Results of the Hydrogen Bonds of Interacting Sets (a−c) at the BP86-D3 (BJ)/Def2-TZVPP Level of Theory (the Values Are in a.u.)

set	interacting hydrogen bond	$\rho(r)$	$\nabla^2\rho(r)$	$H(r)$	$V(r)$	$G(r)$	εBCP	η
a	H19−N9	+0.045	+0.063	−0.010	−0.036	+0.026	+0.007	0.35
b	H25−O5	+0.024	+0.083	−0.00023	−0.020	+0.020	+0.057	0.23
c	H9−O13	+0.033	+0.087	−0.004	−0.029	+0.025	+0.025	0.27

below the plots for each of the interacting sets depict the three-dimensional plots produced by employing sign $(\lambda_2)\rho$. The hydrogen-bonded low-density and low-reduced gradient trough is now negative, indicating an attractive interaction. Conversely, the positive values of the low-density and low-gradient trough point to a repulsive type of interaction. Finally, the dispersion-bound low-density, low-gradient trough is very close to zero.

4. CONCLUSIONS

In this research article, results on the density, speed of sound, and refractive index for three binary liquid mixtures of ethyl lactate with substituted ethanols or ethyl acetate at different temperatures from 298.15 to 323.15 K and at 0.1 MPa have been reported. At the same time, excess volume (V^E), isentropic compressibility (k_s), excess isentropic compressibility (k_s^E), and excess refractive index (n_D^E) were calculated from experimental data and these properties were correlated with the Redlich−Kister equation. The measured excess thermodynamic properties revealed that the molecular interactions in the binary systems follow the order ethyl lactate + 2-aminoethanol > ethyl lactate + ethyl acetate > ethyl lactate + 2-chloroethanol. Also, the FT-IR spectroscopic studies clearly revealed complementary information about the hydrogen bonds between distinct molecules and supported the strength of intra- and intermolecular interactions for three binary systems as per the above suggested trend. Obviously, these excess properties and FT-IR study results provided significant information for a deeper understanding of intra- and intermolecular interactions between unlike molecules in liquid

https://doi.org/10.1021/acs.jced.3c00344
J. Chem. Eng. Data 2024, 69, 1423−1447

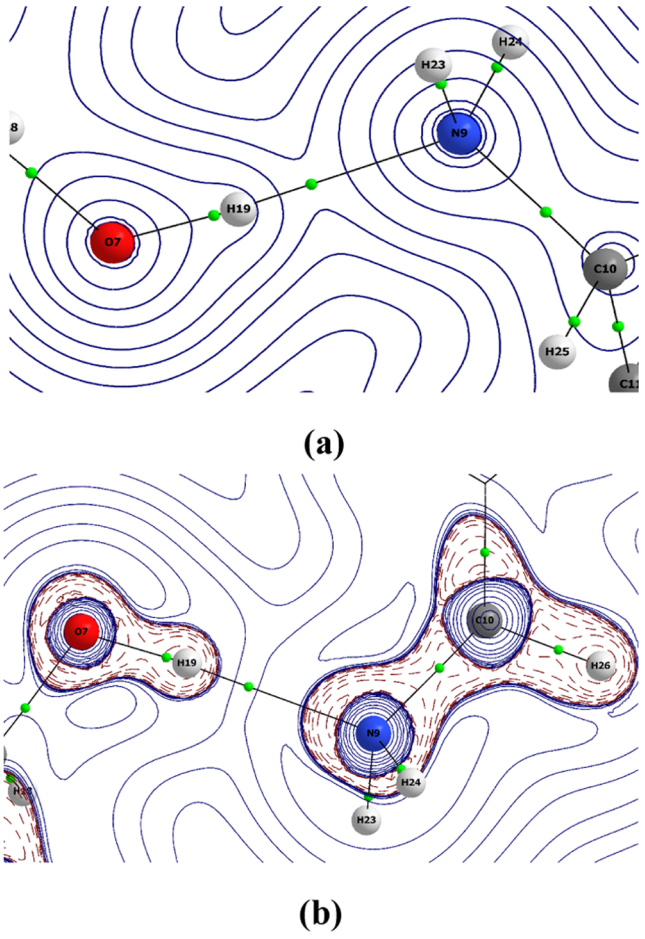

Figure 9. Contour plot of the Laplacian distribution $[\nabla^2 \rho(r)]$ in the O7−H19−N9 plane for the ethyl lactate + 2-aminoethanol interacting set {(a) electron density map $\rho(r)$: contour plot, (b) Laplacian of the electron density map $[\nabla^2 \rho(r)]$: contour plot}. The solid blue lines indicate the areas of charge concentration, while the dotted purple lines represent charge depletion. The solid lines with green spheres are BCPs, which are bond paths, and the thick solid blue lines represent atomic basins indicating the zero-flux crossing surfaces at the molecular plane.

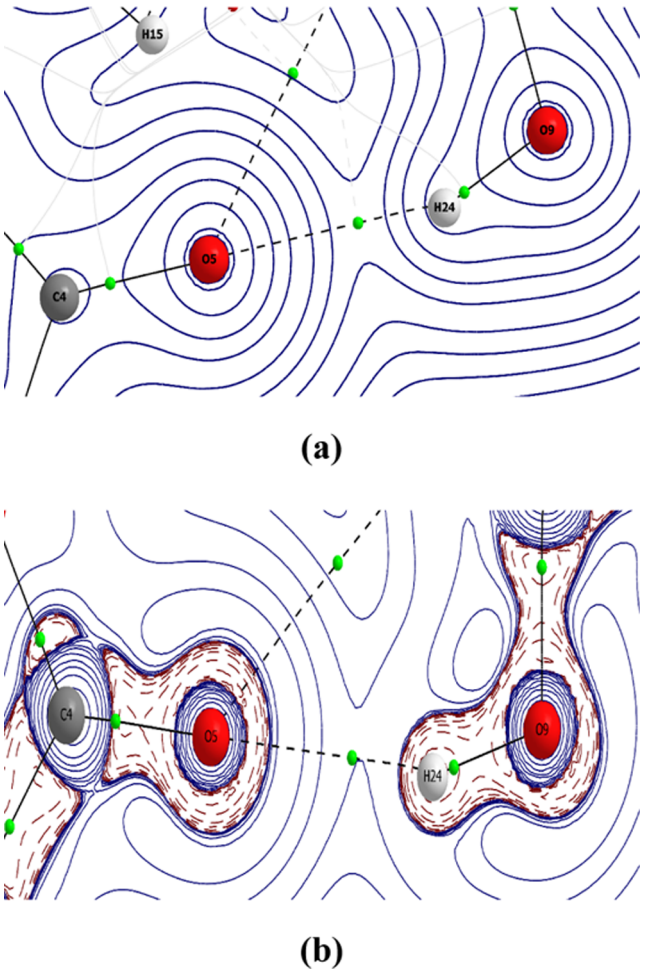

Figure 10. Contour plot of the Laplacian distribution $[\nabla^2 \rho(r)]$ in the O5−H24−O9 plane for the ethyl lactate + 2-chloroethanol interacting set {(a) electron density map $\rho(r)$: contour plot, (b) Laplacian of the electron density map $[\nabla^2 \rho(r)]$: contour plot}. The solid blue lines indicate the areas of charge concentration, while the dotted purple lines represent charge depletion. The solid lines with green spheres are BCPs, which are bond paths, and the thick solid blue lines represent atomic basins indicating the zero-flux crossing surfaces at the molecular plane.

mixtures. Moreover, the computational and QTAIM results provided information about the stabilization energies, hydrogen bonding interactions, and the nature of bonding interactions between the component molecules. From these results, it is observed that stronger interactions are prevailing in the binary system of ethyl lactate and 2-aminoethanol when compared to the other two systems. PC-SAFT was successfully applied to model the density for the three binary mixtures studied in this work (overall deviation = 0.09%). Nomoto's relation coupled to PC-SAFT predicted the speed of sound with a deviation of 1.21%. Finally, it is important to highlight that the four mixing rules used in this work to predict the refractive index were able to correctly model this property, e.g., an overall deviation = 0.04% was obtained with the Lorentz−Lorenz mixing rule.

■ ASSOCIATED CONTENT

Supporting Information

The Supporting Information is available free of charge at https://pubs.acs.org/doi/10.1021/acs.jced.3c00344.

Comparison of experimental density, speed of sound, and refractive index of pure liquids together with available literature data at all of the studies' temperatures (Figure S1) and FT-IR spectra of pure liquids and their mixtures for three binary systems (Figures S2−S4) (PDF)

■ AUTHOR INFORMATION

Corresponding Authors

Indra Bahadur − *Department of Chemistry, North-West University (Mafikeng Campus), Mmabatho 2735, South Africa*; orcid.org/0000-0003-2906-473X; Email: bahadur.indra@nwu.ac.za

Neelam Yugandhar Sreedhar − *Biopolymers and Thermophysical Laboratories, Department of Chemistry, Sri Venkateswara University, Tirupati 517502 Andhra Pradesh, India*; Email: nysthermodynamics@gmail.com

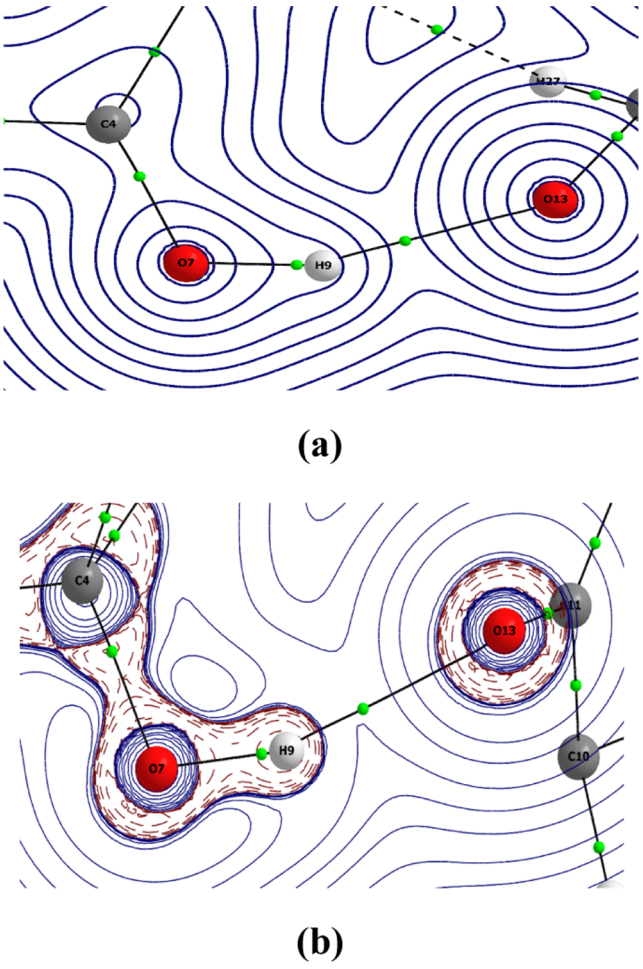

Figure 11. Contour plot of the Laplacian distribution $[\nabla^2 \rho(r)]$ in the O7−H9−O13 plane for the ethyl lactate + ethyl acetate interacting set {(a) electron density map $\rho(r)$: contour plot, (b) Laplacian of the electron density map $[\nabla^2 \rho(r)]$: contour plot}. The solid blue lines indicate the areas of charge concentration, while the dotted purple lines represent charge depletion. The solid lines with green spheres are BCPs, which are bond paths, and the thick solid blue lines represent atomic basins indicating the zero-flux crossing surfaces at the molecular plane.

Authors

Tammisetty Ankaiah − *Biopolymers and Thermophysical Laboratories, Department of Chemistry, Sri Venkateswara University, Tirupati 517502 Andhra Pradesh, India*

Sreenivasulu Karlapudi − *Department of Chemistry, North-West University (Mafikeng Campus), Mmabatho 2735, South Africa;* orcid.org/0000-0003-1319-4417

Shaik Nagulshareef − *Department of Chemistry, Andhra Loyola College, Vijayawada 520008 Andhra Pradesh, India*

Sridhar Battuluri − *Department of Chemistry, S.V. Arts Degree & P.G. College (T.T.D'S), Tirupati 517502 Andhra Pradesh, India*

Doupati Bala Karuna Kumar − *Department of Chemistry, Andhra Loyola College, Vijayawada 520008 Andhra Pradesh, India*

Kasibhatta Siva Kumar − *Department of Chemistry, S.V. Arts Degree & P.G. College (T.T.D'S), Tirupati 517502 Andhra Pradesh, India*

Ariel Hernández − *Departament de Ingeniería Industrial, Facultad de Ingeniería, Universidad Católica de la Santísima Concepción, Concepción 4090541, Chile;* orcid.org/0000-0002-6120-9444

Faruq Mohammad − *Department of Chemistry, College of Science, King Saud University, Riyadh 11451, Kingdom of Saudi Arabia;* orcid.org/0000-0002-9318-9986

Ahmed Abdullah Soleiman − *Department of Chemistry, Southern University and A&M College, Baton Rouge, Louisiana 70813, United States;* orcid.org/0009-0003-2361-8153

Complete contact information is available at: https://pubs.acs.org/10.1021/acs.jced.3c00344

Author Contributions

All authors have equally contributed.

Notes

The authors declare no competing financial interest.

■ ACKNOWLEDGMENTS

The authors wish to express credit to DST-India for awarding Andhra Loyola College with the FIST Programme (SR/FST/College-048/2017) and to the Principal of Andhra Loyola College for providing research lab facilities. The authors wish to acknowledge the North-West University and Sasol. The KSU author acknowledges the funding from the Researchers Supporting Project Number (RSP2024R355), King Saud University, Riyadh, Saudi Arabia.

■ REFERENCES

(1) Ferrari, G.; Foca, G.; Manfredini, M.; Manzini, D.; Marchetti, A.; Tassi, L.; Ulrici, A. Density and Volume Properties of the 2-Chloroethanol + 2-Methoxyethanol + 1,2-Dimethoxyethane Ternary Solvent System at Different Temperatures. *J. Solution Chem.* **2003**, *32*, 93−116.

(2) Karlapudi, S.; Liu, Z.; Bi, Q.; Govinda, V.; Bahadur, I.; Baswanth, O.; Prasad, Ch. Molecular interactions in liquid mixtures containing o-cresol and 1-alkanols: Thermodynamics, FT-IR and computational studies. *J. Mol. Liq.* **2020**, *305*, No. 112798.

(3) Janardhanaiah, M.; Gangadhar, S.; Govinda, V.; Sreenivasulu, K.; Venkateswarlu, P. Effect of alkanol chain length on excess thermodynamic properties of p-cresol with 1-alkanol (C_3−C_8) at 298.15, 303.15, 308.15 and 313.15 K. *J. Mol. Liq.* **2015**, *211*, 169−177.

(4) Karlapudi, S.; Prasad, Ch.; Venkateswarlu, P.; Bahadur, I.; Singh, S.; Ebenso, E. E. Molecular interactions of p-chlorotoluene and 1-alkanols at different temperatures: Volumetric, ultrasonic and FT-IR spectroscopic studies. *J. Mol. Liq.* **2018**, *262*, 302−309.

(5) Karlapudi, Ch. S.; Prasad, L. O.; Olasunkanmi; Singh, S.; Bahadur, I.; Siva Kumar; Ebenso, E. E. Hydrogen Bonding Interactions of m-Chlorotoluene with 1-Alkanol Analyzed by Thermodynamic, Fourier Transform Infrared Spectroscopy, Density Functional Theory, and Natural Bond Orbital. *ACS Omega* **2018**, *3*, 4679−4687.

(6) Kermanpour, H. F.; Niakan, Z. Experimental excess molar properties of binary mixtures of (3-amino-1-propanol + isobutanol, 2-propanol) at T = (293.15 to 333.15) K and modeling the excess molar volume by Prigogine- Flory- Patterson theory. *J. Chem. Thermodyn.* **2012**, *54*, 10−19.

(7) Kermanpour, F.; Sharifi, T. Measurement and correlation of the excess properties of ternary mixture of {x1[Hmim][BF4] + x21-propanol + x32-propanol} at different temperatures. *J. Chem. Eng. Data* **2014**, *59*, 1922−1929.

(8) Kermanpour, F.; Ettefagh, S. T.; Iloukhani, H. Measurement and calculation the excess molar properties of binary mixtures containing isobutanol, 1-amino-2-propanol, and 1-propanol at temperatures of (293.15 to 333.15) K. *J. Solution Chem.* **2017**, *46*, 446−460.

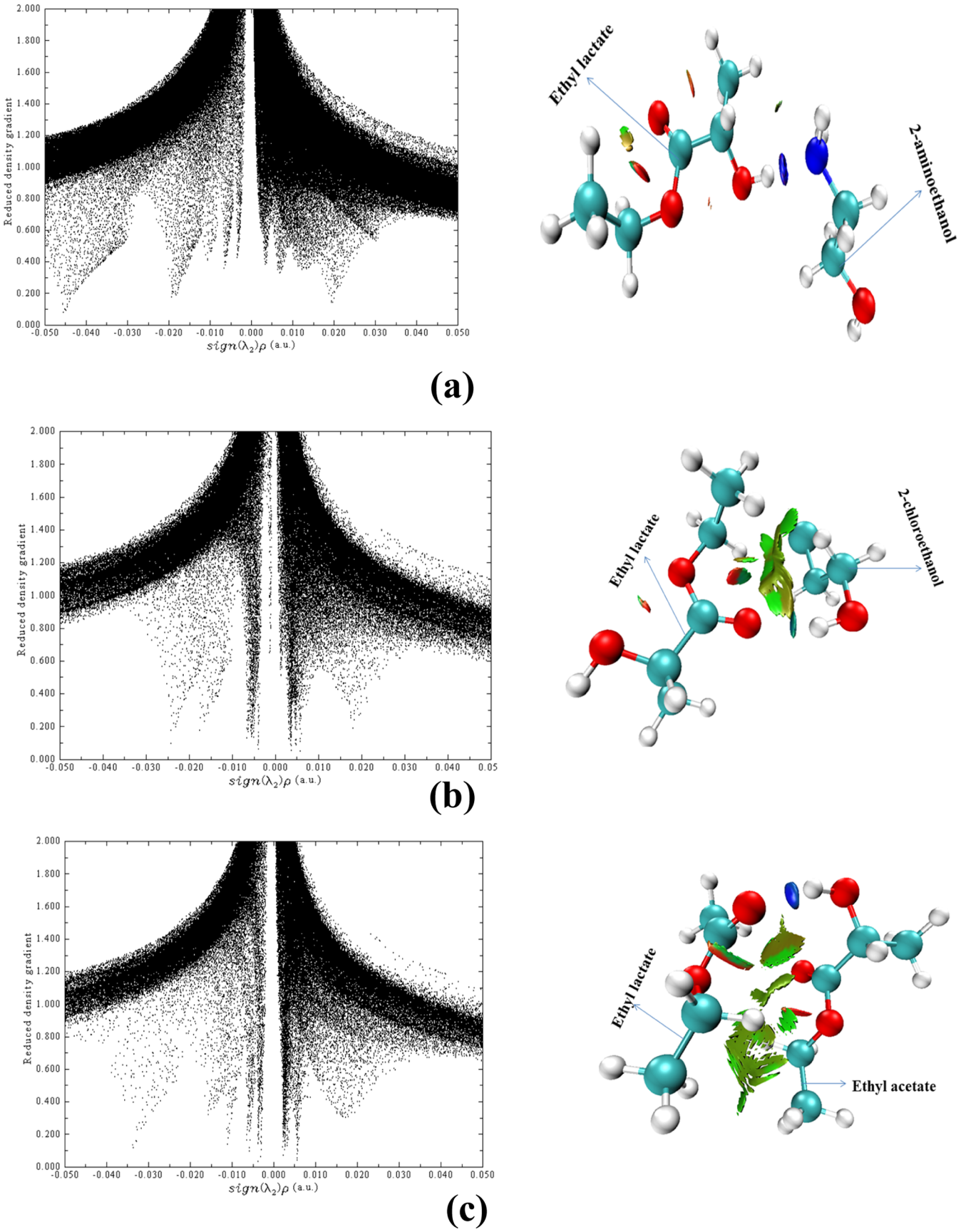

Figure 12. Plots of the reduced density gradient versus the electron density multiplied by the sign of the second Hessian eigenvalues and gradient isosurfaces with s = 0.5 a.u. for the three interacting sets (a) ethyl lactate + 2-aminoethanol, (b) ethyl lactate + 2-chloroethanol, and (c) ethyl lactate + ethyl acetate. The colors represent the following: blue: hydrogen bonding interaction, green: attractive electrostatic interaction, and red: repulsive interaction. The colors are based on product values of (sign) (second Hessian eigenvalue) (electron density) ranging from −0.03 to 0.02 a.u.

https://doi.org/10.1021/acs.jced.3c00344
J. Chem. Eng. Data 2024, 69, 1423−1447

(9) Sanchez, J.; Artigas, H.; Gascon, I.; Lafuente, C. Thermodynamic behaviour of alkyl lactate-alkanol systems. *J. Chem. Thermodyn.* **2018**, *127*, 33−38.
(10) Bayless, R. E. Graphic Ink Remover Solution. US5,464,555 A.1995.
(11) Guo, H.; Wang, W.; Sun, Y.; Li, H.; Ai, F.; Xie, L.; Wang, X. Ethyl lactate enhances ethylenediaminedisuccinic acid solution removal of copper from contaminated soils. *J. Hazard. Mater.* **2010**, *174*, 59−63.
(12) Aminabhavi, T. M.; Phayde, H. T.; Khinnavar, R. S.; Gopalakrishna, B.; et al. Densities, refractive indices, speeds of sound, and shear viscosities of diethylene glycol dimethyl ether with ethyl acetate, methyl benzoate, ethyl benzoate, and diethyl succinate in the temperature range from 298.15 to 318.15 K. *J. Chem. Eng. Data* **1994**, *39* (2), 251−260, DOI: 10.1021/je00014a014.
(13) Xu, Li.; Lin, G.; Wang, Xu.; Lin, R. Densities and volumetric properties of 2-chloroethanol with N,N-dimethylformamide and water at different temperatures. *J. Mol. Liq.* **2006**, *123*, 130−133.
(14) Roderich, R.; Corbett, J. F. *Ullmann's Encyclopedia of Industrial Chemistry*; Wiley-VCH: New York (NY), 2002.
(15) Mukesh, B.; Sreekanth, T.; Srinivasa Krishna, T.; Gowrisankar, M. Thermodynamic and transport properties of 2- methoxyaniline with substituted ethanols at various temperatures. *Int. J. Ambient Energy* **2022**, *43*, 425−434, DOI: 10.1080/01430750.2019.1636873.
(16) Anila, P.; Reddy, K. R.; Rao, G. S.; Sairam, P. V.; Ramachandran, D.; et al. Densities, speed of sound, and IR studies of Ethyl lactate with 2-alkoxyethanols at different temperatures. *Thermochim. Acta* **2015**, *620*, 1−9, DOI: 10.1016/j.tca.2015.09.021.
(17) VaniLatha, S.; Little Flower, G.; Rayapa Reddy, K.; NageswaraRao, C. V.; Ratnakar, A. Exploration of volumetric, acoustic, thermodynamic and IR studies of binary mixtures of green solvent ethyl lactate with C_3alkanols at T = (303.15, 308.15, 313.15 and 318.15) K and atmospheric pressure. *J. Mol. Liq.* **2015**, *209*, 153−160.
(18) Anila, P.; Rayapa Reddy, K.; SrinivasaRao, G.; Sairam, P. V. S.; Ramachandran, D.; Rambabu, C. Comparative studies of intermolecular interaction of aromatic amines with ethyl lactate at different temperatures. *J. Chem. Thermodyn.* **2017**, *104*, 24−32.
(19) Shakila, A.; Ravikumar, S.; Raveendra, M.; Sivakumar, K.; Raju, R.; Pandiyan, V. Thermodynamic and FT-IR study on molecular interactions between ethyl lactate with alkyl amines at different temperatures. *Phys. Chem. Liq.* **2018**, *57* (1), 117−136, DOI: 10.1080/00319104.2018.1432047.
(20) Grande, M. D.; Álvarez Juliá, J.; Barrero, C. R.; Marschoff, C. M. Insight into the binary mixture of ethyl lactate + acetonitrile from density, speed of sound and refractive index measurements. *Phys. Chem. Liq.* **2019**, *57* (2), 151−162, DOI: 10.1080/00319104.2018.1432050.
(21) Grandea, M. C.; Álvarez Juliá, J.; Barreroa, C. R.; Marschof, C. M. Density, speed of sound, refractive index and related properties of the binary mixture ethyl lactate + butyronitrile at various temperatures. *Phys. Chem. Liq.* **2021**, *59* (3), 467−479, DOI: 10.1080/00319104.2020.1737865.
(22) Resa, J. M.; Goenaga, J. M.; Sanchez-Ruiz, A. I.; Iglesias, M. Density, Refractive Index, Speed of Sound at 298.15 K, and Vapor-Liquid Equilibria at 101.3 kPa for Binary Mixtures of Ethyl Acetate + Ethyl Lactate and Methyl Acetate + Ethyl Lactate. *J. Chem. Eng. Data* **2006**, *51*, 1294−1299.
(23) Ayad, A.; Belabbaci, A.; Negadi, A.; Hernández, A.; Kabane, B.; Bahadur, I.; Faruq Mohammad, F.; Soleiman, A. A.; Negadi, L. Measurements and Modeling of Thermodynamic Properties of Binary Systems Comprising (2-Amino-2-methyl-1-propanol with Acetonitrile, Toluene, 1-Pentanol or 1-Hexanol) at Different Temperatures. *J. Chem. Eng. Data* **2023**, *68* (11), 2789−2806, DOI: 10.1021/acs.jced.2c00767.
(24) Bajić, D. M.; Živković, E. M.; et al. Experimental measurements and modelling of volumetric properties, refractive index and viscosity of binary systems of ethyl lactate with methyl ethyl ketone, toluene and n-methyl-2-pirrolidone at 288.15 to 323.15 K and atmospheric pressure. New UNIFAC-VISCO and ASOG-VISCO interaction parameters. *Fluid Phase Equilib.* **2015**, *399*, 50−65, DOI: 10.1016/j.fluid.2015.04.017.
(25) Yasmin, M.; Gupta, M. Density, Viscosity, Velocity and Refractive Index of Binary Mixtures of Poly(Ethylene Glycol) 200 with Ethanolamine, m-Cresol and Aniline at 298.15 K. *J. Solution Chem.* **2011**, *40*, 1458−1472.
(26) Resa, J. M.; Cepeda, E. A.; Goenaga, J. M.; Ramos, A.; Aguirre, S.; Urbano, C. Density, Refractive Index, Speed of Sound at 298.15 K, and Vapor-Liquid Equilibrium at 101.3 kPa for Binary Mixtures of Methanol + Ethyl Lactate and 1-Propanol + Ethyl Lactate. *J. Chem. Eng. Data* **2010**, *55*, 1017−1021.
(27) Aralaguppi, M. I.; Jadar, C. V.; Aminabhavi, T. M. Density, Viscosity, Refractive Index, and Speed of Sound in Binary Mixtures of 2-Chloroethanol with Methyl Acetate, Ethyl Acetate, n-Propyl Acetate, and n-Butyl Acetate. *J. Chem. Eng. Data* **1999**, *44*, 441−445.
(28) Aminabhavi, T. M.; Banerjee, K. Density, Viscosity, Refractive Index, and Speed of Sound in Binary Mixtures of 2-Chloroethanol with Alkanols (C1-C6) at 298.15, 303.15, and 308.15 K. *J. Chem. Eng. Data* **1998**, *43*, 509−513.
(29) Baragi, J. G.; Aralaguppi, M. I.; Aminabhavi, T. M.; Kariduraganavar, M. Y.; Kittur, A. S. Density, Viscosity, Refractive Index, and Speed of Sound for Binary Mixtures of Anisole with 2-Chloroethanol, 1,4-Dioxane, Tetrachloroethylene, Tetrachloroethane, DMF, DMSO, and Diethyl Oxalate at (298.15, 303.15, and 308.15) K. *J. Chem. Eng. Data* **2005**, *50*, 910−916.
(30) Pandey, P. K.; Awasthi, A.; Awasthi, A. Acoustic, volumetric and spectroscopic properties of formamide + N-methylformamide + 2-chloroethanol at different temperatures. *Phys. Chem. Liq.* **2014**, *52*, 320−330.
(31) Pandey, P. K.; Awasthi, A.; Awasthi. Intermolecular interactions in binary mixtures of 2-Chloroethanol with 2-Dimethylaminoethanol and 2-Diethylaminoethanol at different temperatures. *Chem. Phys.* **2013**, *423*, 119−126.
(32) Álvarez, E.; Cerdeira, F.; Gomez-Diaz, D.; Navaza, J. M. Density, Speed of Sound, Isentropic Compressibility, and Excess Volume of (Monoethanolamine + 2-Amino-2-methyl-1-propanol), (Monoethanolamine + Triethanolamine), and (Monoethanolamine + N-Methyldiethanolamine) at Temperatures from (293.15 to 323.15) K. *J. Chem. Eng. Data* **2010**, *55*, 994−999.
(33) Li, Z.; Zhao, D.; Zhuang, Y.; Yang, F.; Liu, X.; Chen, Y. Volumetric properties of monoethanolamine and alcohol binary mixtures at different temperatures and 0.1 MPa. *J. Chem. Thermodyn.* **2019**, *133*, 37−45.
(34) Blanco, A.; Garcia-Abuin, A.; Gomez-Diaz, D.; Navaza, J. M.; Villaverde, O. L. Density, Speed of Sound, Viscosity, Surface Tension, and Excess Volume of N-Ethyl-2-pyrrolidone + Ethanolamine (or Diethanolamine or Triethanolamine) from T = (293.15 to 323.15) K. *J. Chem. Eng. Data* **2013**, *58*, 653−659.
(35) Nallani, S.; Boodida, S.; Tangeda, S. J. Density and Speed of Sound of Binary Mixtures of N-Methylacetamide with Ethyl Acetate, Ethyl Chloroacetate, and Ethyl Cyanoacetate in the Temperature Interval (303.15 to 318.15) K. *J. Chem. Eng. Data* **2007**, *52*, 405−409.
(36) Sarkar, L.; Roy, M. N. Studies on Liquid−Liquid Interactions of Some Ternary Mixtures by Density, Viscosity, Ultrasonic Speed and Refraction Index Measurements. *Thermochim. Acta* **2009**, *496*, 124−128.
(37) Majstorović, D.; Mirković, M. R.; Kijevčanin, M.; Živković, E. Analysis of thermophysical properties of binary systems containing ethyl acetate and 1-propanol or 1-butanol. *Hem. Ind.* **2020**, *74* (3), 163−185, DOI: 10.2298/HEMIND191203017M.
(38) Gross, J.; Sadowski, G. Perturbed-chain SAFT: An equation of state based on a perturbation theory for chain molecules. *Ind. Eng. Chem. Res.* **2001**, *40*, 1244−1260.
(39) Gross, J.; Sadowski, G. Application of the perturbed-chain SAFT equation of state to associating systems. *Ind. Eng. Chem. Res.* **2002**, *41*, 5510−5515.

(40) Kleiner, M.; Sadowski, G. Modeling of polar systems using PCP-SAFT: An approach to account for induced-association interactions. *J. Phys. Chem. C* **2007**, *111*, 15544−15553.
(41) Nomoto, O. Empirical formula for sound velocity in liquid mixtures. *J. Phys. Soc. Jpn.* **1958**, *13*, 1528−1532.
(42) Giner, B.; Lafuente, C.; Villares, A.; Haro, M.; López, M. C. Volumetric and refractive properties of binary mixtures containing 1, 4-dioxane and chloroalkanes. *J. Chem. Thermodyn.* **2007**, *39*, 148−157.
(43) (a) Mitoraj, M.; Michalak, A. Donor−acceptor properties of ligands from the natural orbitals for chemical valence. *Organometallics* **2007**, *26*, 6576−6580, DOI: 10.1021/om700754n. (b) Mitoraj, M.; Michalak, A. Applications of natural orbitals for chemical valence in a description of bonding in conjugated molecules. *J. Mol. Model.* **2008**, *14*, 681−687, DOI: 10.1007/s00894-008-0276-1. (c) TeVelde, G.; Bickelhaupt, F. M.; Baerends, E. J.; Fonseca Guerra, C.; van Gisbergen, S. J. A.; Snijders, J. G.; Ziegler, T. Chemistry with ADF. *J. Comput. Chem.* **2001**, *22*, 931−967, DOI: 10.1002/jcc.1056. (d) Van Lenthe, E.; Baerends, E. J. Optimized Slater-type basis sets for the elements 1−118. *J. Comput. Chem.* **2003**, *24*, 1142−1156, DOI: 10.1002/jcc.10255. (e) Lenthe, E. V.; Baerends, E. J.; Snijders, J. G. Relativistic regular two-component Hamiltonians. *J. Chem. Phys.* **1993**, *99*, 4597−4610, DOI: 10.1063/1.466059. (f) van Lenthe, E.; Baerends, E. J.; Snijders, J. G. Relativistic total energy using regular approximations. *J. Chem. Phys.* **1994**, *101* (11), 9783−9792, DOI: 10.1063/1.467943. (g) Zhao, L.; von Hopffgarten, M.; Andrada, D. M.; Frenking, G.*WIREs Comput. Mol. Sci.* 2018; Vol. *8*, pp 1345−1382. (h) Zhao, L.; Hermann, M.; Schwarz, W. H. E.; Frenking, G. The Lewis electron-pair bonding model: modern energy decomposition analysis. *Nat. Rev. Chem.* **2019**, *3*, 48−63, DOI: 10.1038/s41570-018-0060-4. (i) Andrés, J.; Ayers, P. W.; Boto, R. A.; Carbó-Dorca, R.; Chermette, H.; Cioslowski, J.; Contreras-García, J.; Cooper, D. L.; Frenking, G.; Gatti, C.; Heidar-Zadeh, F.; Joubert, L.; Martín Pendás, Á.; Matito, E.; Mayer, I.; Alston, J.; Misquitta, Y.; Mo, J.; Pilmé, P. L. A.; Popelier, M.; Rahm. Nine questions on energy decomposition analysis. *J. Comput. Chem.* **2019**, *40*, 2248−2283.
(44) Becke, A. D. A Multicenter Numerical Integration Scheme for Polyatomic Molecules. *J. Chem. Phys.* **1988**, *88*, 2547−2553.
(45) Franchini, M.; Philipsen, P. H.; Visscher, L. The Becke Fuzzy Cells Integration Scheme in the Amsterdam Density Functional Program Suite. *J. Comput. Chem.* **2013**, *34*, 1819−1827.
(46) Peña-Tejedor, S.; Murga, R.; Sanz, M. T.; Beltran, S. Vapor−liquid equilibria and excess volumes of the binary systems ethanol + ethyl lactate, isopropanol + isopropyl lactate and n-butanol + n-butyl lactate at 101.325 kPa. *Fluid Phase Equilib.* **2005**, *230*, 197−203.
(47) Benson, G. C.; Kiyohara, G. C. Evaluation of excess isentropic compressibilities and isochoric heat capacities. *J. Chem. Thermodyn.* **1979**, *11*, 1061−1064.
(48) Douheret, G.; Moreau, C.; Viallard, A. Excess thermodynamic quantities in binary systems of non-electrolytes: Different ways of calculating excess compressibilities. *Fluid Phase Equilib.* **1985**, *22* (3), 277−287, DOI: 10.1016/0378-3812(85)87027-8.
(49) Riddick, J. A.; Bunger, W. B.; Sakano, T. K. *Organic Solvents Physical Properties and Methods of Purification*, 4th ed.; Wiley Interscience: New York, 1986.
(50) Zábranský, M.; Ruzicka, V., Jr. Estimation of the heat capacities of organic liquids as a function of temperature using group additivity: an amendment. *J. Phys. Chem. Ref. Data* **2004**, *33*, 1071−1081.
(51) Deshpande, D. D.; Patterson, D.; Andreoli-Ball, L.; Costas, M.; Trejo, L. M. Heat Capacities, Selfassociation and Complex Formation in Alcohol-Ester Systems. *J. Chem. Soc. Faraday Trans.* **1991**, *87*, 1133−1139.
(52) Zábranský, M.; Hynek, V.; Finkeova-Hastabova, J.; Vesely, F. Heat Capacities of Six Liquid Esters as a Function of Temperature. *Collect. Czech. Chem. Commun.* **1987**, *52*, 251−257.
(53) Reis, J. C. R.; Lampreia, I.; Santos, A. F.; Moita, M. L.; Douheret, G. Refractive index of liquid mixtures: theory and experiment. *ChemPhysChem* **2010**, *11*, 3722−3733.
(54) Redlich, O.; Kister, A. T. Algebraic representation of thermodynamic properties and the classification of solutions. *Ind. Eng. Chem.* **1948**, *40*, 345−348.
(55) Daubert, T. E.; Danner, R. P. *Physical and Thermodynamic Properties of Pure Chemicals: Data Compilation*; Taylor & Francis: Bristol, PA, 2004.
(56) Espinosa, E.; Alkorta, I.; Elguero, J.; Molins, E. From weak to strong interactions: A comprehensive analysis of the topological and energetic properties of the electron density distribution involving X−H···F−Y systems. *J. Chem. Phys.* **2002**, *117*, 5529−5542.
(57) Vener, M. V.; Manaev, A. V.; EgorovaA, N.; Tsirelson, V. G. QTAIM Study of Strong H-Bonds with the O−H···A Fragment (A = O, N) in Three-Dimensional Periodical Crystals. *J. Phys. Chem. A* **2007**, *111*, 1155−1162.
(58) Gatti, C.; Kristallogr, Z. *Chemical Bonding in Crystals: New Directions*; De Gruyter, 2005; Vol. *220*, pp 399−457.
(59) Grabowski, S. J. What Is the Covalency of Hydrogen Bonding? *Chem. Rev.* **2011**, *111*, 2597−2625.
(60) Gervasio, G.; Bianchi, R.; Marabello, D. About the topological classification of the metal−metal bond. *Chem. Phys. Lett.* **2004**, *387*, 481−484.
(61) Bader, R. F. W. *Encyclopedia of Computational Chemistry*; John Wiley Sons Inc.: La Jolla, 1998.
(62) Jordan, D.; Smith, P. *Mathematical Techniques: An Introduction for the Engineering, Physical, and Mathematical Sciences*, 2nd ed.; OUP Oxford, 2008; Vol. *67*, pp 165−169.
(63) Bader, R. F. W.; Essen, H. The characterization of atomic interactions. *J. Chem. Phys.* **1984**, *80*, 1943−1960.